# Tyre Pressure Monitoring using Sensors

Tove Bergdahl

| **Department of Automatic Control** **Lund Institute of Technology** **Box 118** **SE-221 00 Lund Sweden** | *Document name* MASTER THESIS |
| --- | --- |
| | *Date of issue* April 2007 |
| | *Document Number* ISRNLUTFD2//TFRT--5790--SE |

| *Author(s)* Tove Bergdahl | *Supervisor* Magnus Rau at Daimler Chrysler in Germany Karl-Erik Årzén at Automatic Control in Lund |
| --- | --- |
| | *Sponsoring organization* |

*Title and subtitle*
Tyre Pressure Monitoring using Sensors (Övervakning av däckstryck med sensorer)

*Abstract*

This Master Thesis analysis an indirect tyre pressure monitoring system for passenger cars under the influence of warp. Warp is the manipulation of the handling properties of a vehicle which can be used in driver assistance applications. Driving with warp affects the tyre pressure monitoring system such that false warning for a deflated tyre can occur. An explanation to the false warnings is presented, as well as a possible method of compensation for warp which can be implemented in the tyre pressure monitoring algorithm. Finally a different type of indirect pressure monitoring system, which involves observing changes in the eigen frequency of the unsprung mass of the vehicle, is presented and evaluated.

*Keywords*

*Classification system and/or index terms (if any)*

*Supplementary bibliographical information*

*The report may be ordered from the Department of Automatic Control or borrowed through:University Library, Box 3, SE-221 00 Lund, Sweden Fax +46 46 222 42 43*

# Preface

First of all, I would like to thank Professor Karl-Erik Årzén at the Department of Automatic Control, Lund University, for setting up the contact with Daimler Chrysler in Stuttgart and thereby giving me the opportunity to do my Master Thesis there. I would also like to thank my supervisor at Daimler Chrysler, Magnus Rau, for formulating my thesis project and for great support and guidance throughout my work.

# Contents

# List of Tables

# List of Figures

# Chapter 1

# Introduction

This chapter gives a thorough introduction to the project for this Master Thesis. First, in Section 1.1, a motivation for the topic is given followed by some background knowledge in Section 1.2. The overall objective of the project is presented in Section 1.3. In Section 1.4 the thesis is divided up into tasks and corresponding suggestions for solution of the tasks is given in Section 1.5.

## 1.1  Motivation

The tyres are the sole part of the vehicle which have contact with the road surface. Thus, their quality is of great importance for safe driving. Even though tyres are brand new, driving with insufficient pressure will have several negative effects on safety. Steering properties worsen, there is a higher risk of hydro planning and the stopping distance is increased. There are also economical and environmental effects, fuel consumption will increase and tyres are worn down faster. Of course there is the most obvious risk of having a flat tyre, which not only can be dangerous but also damaging to the car.

Tyres can be underinflated due to two reasons, damage or natural diffusion. Natural diffusion rate is around 0.1 bar per month [1] and therefore tyres need to be checked properly on a regular basis. Often this is not done, resulting in a substantial number of vehicles on the road with insufficient tyre pressure. Hence, there is a need for a reliable tyre pressure monitoring system, TPMS, in all vehicles.

## 1.2  Problem background

### 1.2.1  Indirect and direct methods

There are two major approaches to tyre pressure monitoring, direct monitoring and indirect monitoring. The direct method uses a sensor which measures pressure and temperature directly in the tyre cavity [2]. Indirect pressure monitoring systems takes already provided sensor signals, usually from the ABS [1] system, and use these to derive a relative pressure value. There exists several suggested solutions to indirect monitoring.

The major advantage with direct pressure monitoring is that the results are in general more exact than any indirect method and thus less probable to give false warnings. There

---

[1] Anti-lock Braking System

is also the possibility to detect an equal loss of pressure in all four wheels at the same time, which most existing indirect methods can not do since they rely on relative pressure estimates. Also, a direct method can normally detect pressure loss faster than an indirect method.

As good as this sounds, direct methods do have some disadvantages. The main one is that implementation costs are a lot higher than for the indirect method. To install this system, four modules, each with pressure and temperature sensors and a transmitter, must be fitted correctly in the tyre cavity. A communication network must be set up with a central unit with a receiver to gather all information from the four tyres. Each module also needs long-lasting power supply. Existing systems use a durable type of battery, constructed to cope with the harsh environment in the tyre cavity.

The indirect method, on the other hand, uses already existing sensor signals and requires only a software upgrade, assuming the car is equipped with an ABS system. Also the system is practically maintenance-free, in contrast to the direct system which could meet problems with hardware failure and which also needs special attention in the case of a tyre change.

### 1.2.2 Brief description of existing Tyre Pressure Monitoring System

The current indirect TPMS in some of the Mercedes cars is the Warnair DWS [2]. The system is also called the PRW, Plattrollwarner, which will be the term used in this report. This is a system which uses the most common indirect method of monitoring tyre pressure today. The method uses the relationship between tangential velocity at each wheel and angular wheel speed:

$$\omega_i = \frac{v_{x,i}}{r_{dyn,i}} \tag{1.1}$$

$i = 1...4$ (see Figure 1.1), where $\omega$ is angular wheel speed, $v_x$ is velocity and $r_{dyn}$ is the dynamic radius.

An underinflated tyre has a smaller radius than a correctly inflated tyre and the angular wheel speed of an underinflated tyre will thus be faster than the other tyres. Somewhat simplified, a low tyre pressure is detected by comparing the wheel speeds of all four wheels. There exists however some particular cases when this method can give false warnings, for example, during strong lateral acceleration or heavy braking. To prevent false warnings the PRW algorithm can therefore identify these situations and compensate for them. The PRW is further described in Section 2.1.

### 1.2.3 Warp

Warp is the altering of a vehicle's direction of motion without actually changing the steering wheel angle. This is performed by manipulating the wheel loads such that torque equilibrium remains around the vertical and longitudinal axis but net load on the individual wheel will change, making the vehicle turn. See Figure 1.2 and Equation 1.2. The wheel loads are changed through the ABC [3] system. This is an active suspension system aimed to dampen the vehicle's body movements by controlling the vertical forces at each wheel. Warp is described as:

$$warp = F_{z,1} - F_{z,2} - F_{z,3} + F_{z,4} \tag{1.2}$$

---

[2] Deflation Warning System
[3] Active Body Control
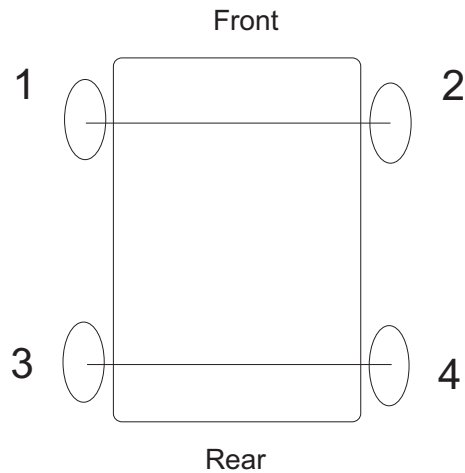
Figure 1.1: Basic car illustrating numbering of wheels.

where $F_{z,i}$, $i = 1...4$ are the wheel loads for each wheel respectively.
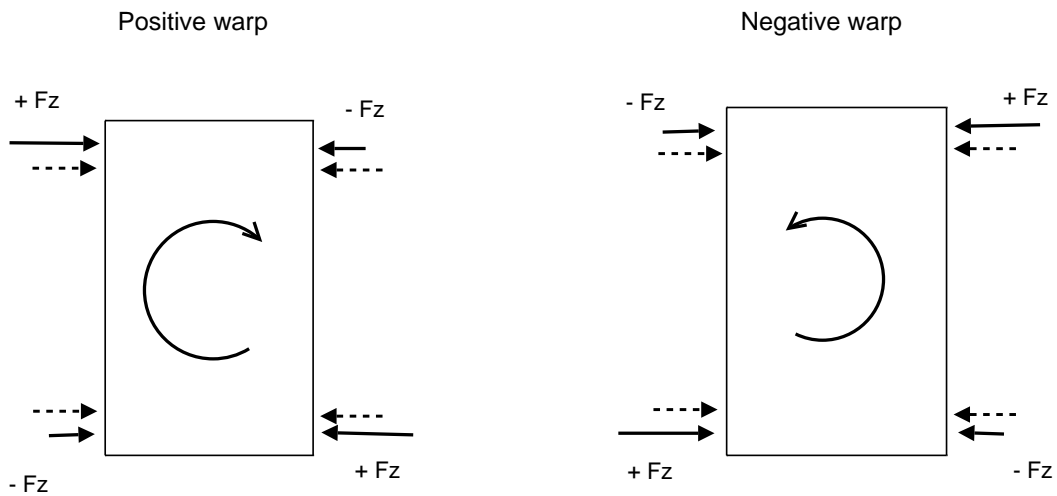


Figure 1.2: Overview of positive and negative warp. The dotted arrows represent normal wheel load.

Since warp influences the handling properties of the vehicle it can be used to assist the driver with, for example, lane-keeping and road bank. Chapter 5 brings up more about warp and these two applications.

### 1.2.4 Warp's influence on the PRW

When driving with constant warp, the PRW will incorrectly warn for low tyre pressure. Warp alters the wheel loads, in order to make the vehicle turn, at the same time causing a change in dynamic radius of the tyres which affects the wheel speeds, see Equation 1.1. Since the PRW relies on the wheel speeds for low tyre pressure warning, driving with warp will affect the system and can cause false warnings. The PRW algorithm already compensates for some driving situations which could incorrectly trigger a warning and it is evident that some sort

of compensation is needed for driving with warp as well. The influence on the PRW due to warp will be fully investigated in Chapter 3.

## 1.3 Objective

The goal for this Master Thesis is to design a tyre pressure monitoring system that will function correctly while driving with warp. It is desirable that the system is reliable and does not issue false warnings. Even though a false warning is not in itself something critical, it will lead to lack of trust for the system and eventually end-users will start to ignore the warning.

## 1.4 Problem definition

1. Establish the relationship between wheel load and dynamic radius, explaining why the PRW can incorrectly issue a warning when driving with warp.

2. Suggest a compensation strategy for warp and analyse the benefits of this compensation as a part of the PRW algorithm.

3. Find an alternative method for tyre pressure monitoring and investigate how this could be used successfully instead of the current TPMS.

## 1.5 Suggested solution

1. Study software description of current system and measurements from test track with different warp levels. Analyse the relationship between wheel load, dynamic radius and other important variables.

2. Develop a warp compensation using the results from the analysis. Build a Simulink model containing the basic logic of the PRW and simulate with field measurements, captured with a real vehicle. Analyse the affect on the PRW due to warp and the benefits of the compensation.

3. The alternative method chosen for tyre pressure monitoring is:

   - Resonance frequency method: Observing the change of the resonance frequency of the unsprung mass [4] caused by deflation of tyre.

### 1.5.1 Equipment and work method

All work has been performed at Daimler Chrysler in Stuttgart, Germany. The software used throughout the project is Matlab and the models are built in Simulink. All field measurement capturing and testing have been done on a test track with a Mercedes S-class vehicle equipped with ABS, ABC, ESP [5] and warp. The tyres used are Continental Sport Contact 2 with the dimensions 255/40 R19 96Y for the front tyres and 275/40 101Y for the rear tyres.

---

[4]Everything not carried by the suspension, i.e. wheels, tyres, brakes, axles and components belonging to the suspension

[5]Elektronisches Stabilitäts Programm, Electronic Stability Control

# Chapter 2

# The PRW algorithm

In this chapter the PRW algorithm is described in more detail. Section 2.1 explains how the PRW strategy works and Section 2.2 discusses some of the limitations of the PRW functionality. Finally, the corrections and data rejections made in the algorithm are brought up in Section 2.3 and 2.4 respectively.

## 2.1 Tyre pressure monitoring strategy

As mentioned in the introduction, the PRW uses the angular wheel speed signals from the ABS system in order to detect a low tyre pressure. The main principle is that if one wheel is incorrectly inflated it will turn faster than the other wheels due to the relationship between the tangential velocity at each wheel, the individual angular wheel speeds and the dynamic radius of the tyre, see Equation 1.1.

Tyre deflation is recognized by comparison of three different variables [3],

- $diag$ – Evaluation of wheel speeds diagonal to each other.

- $fr$ – Front/rear wheel speeds.

- $lr$ – Left/right wheel speeds.

according to Equations 2.1, 2.2, 2.3 and Figure 2.1.

$$diag \quad = \quad (\frac{\omega_1 + \omega_4}{\omega_2 + \omega_3} - 1) \cdot 100 \tag{2.1}$$

$$fr \quad = \quad (\frac{\omega_1 + \omega_2}{\omega_3 + \omega_4} - 1) \cdot 100 \tag{2.2}$$

$$lr \quad = \quad (\frac{\omega_1 + \omega_3}{\omega_2 + \omega_4} - 1) \cdot 100 \tag{2.3}$$

The $diag$ variable is really the true indicator for tyre deflation. If its value exceeds a certain threshold, a warning could be triggered. The exact threshold value varies depending on the vehicle. Whether the warning is set or not depends on $fr$ and $lr$, which act as safety variables to
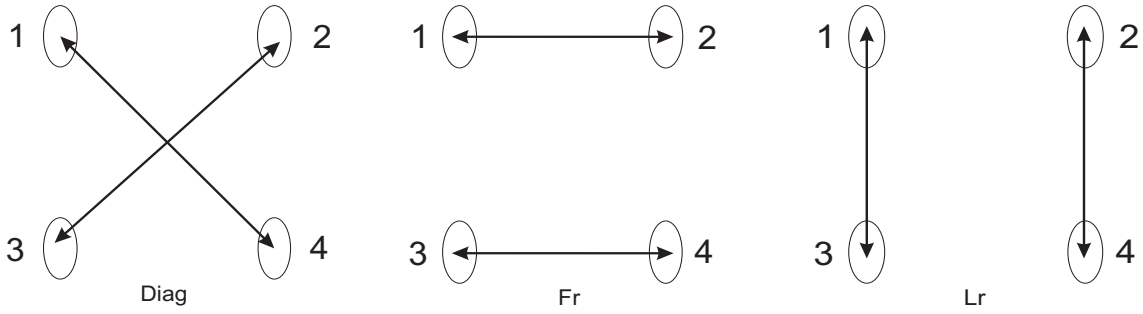
Figure 2.1: Illustration of how the wheel speeds that constitute the PRW variables are picked.

prevent false warnings. The PRW warning strategy is presented in Table 2.1. The *thr* variable stands for the threshold value associated with the *diag* variable. The *FL* variable stands for the deflation warning concerning the Front Left tyre, the *FR* variable for the deflation warning concerning the Front Right tyre, the *RL* variable for the deflation warning concerning the Rear Left tyre and the *RR* variable for the deflation warning concerning the Rear Right tyre. Should the values of all three variables *diag*, *fr* and *lr*, at one point in time, match any of the cases *FL*, *FR*, *RL* or *RR*, a warning will be issued.

If all angular wheel speeds are the same the variables *diag*, *fr* and *lr* should be equal to zero meaning that none of the conditions in any of the cases for deflation warning seen in Table 2.1 are fulfilled and thus no warning is issued. If, for example, the rear left tyre is deflated the value of the *diag* and *fr* variable will decrease below zero, and the *lr* variable will increase above zero which will, according to Table 2.1, cause the *RL* warning to be triggered.

Table 2.1: PRW warning strategy, *thr* = threshold value.

|  | *FL* | *FR* | *RL* | *RR* |
|---|---|---|---|---|
| *diag* | $> thr$ | $< -thr$ | $< -thr$ | $> thr$ |
| *fr* | $> 0$ | $> 0$ | $< 0$ | $< 0$ |
| *lr* | $> 0$ | $< 0$ | $> 0$ | $< 0$ |

## 2.2 Limits of the algorithm

With an indirect tyre pressure monitoring system, such as the PRW, the possibility of detecting a pressure loss depends on how many tyres that are deflated and by how much.

### 2.2.1 One tyre deflated

The PRW algorithm can detect if one tyre is deflated by around 30% or more. For example, if the front right tyre is deflated, its angular wheel speed will increase compared to the other tyres and evoke a change of the PRW variables as:

$$
\left.\begin{array}{ll}
\omega_1 & \rightarrow \\
\omega_2 & \uparrow \\
\omega_3 & \rightarrow \\
\omega_4 & \rightarrow
\end{array}\right\} \implies \left.\begin{array}{ll}
diag & \downarrow \\
fr & \uparrow \\
lr & \downarrow
\end{array}\right\} \Rightarrow \text{FR warning}
$$

where $\omega_i$ is the angular wheel speed for the i:th wheel. See Table 2.1 for how the change in the PRW variables caused by the deflation generates the *FR* warning.

This behaviour can also be seen in Figure 2.2 which illustrates how the *diag*, *fr* and *lr* behave with one underinflated tyre. Here, the angular wheel speeds from a measurement captured with the front right tyre of the vehicle around 50% deflated, have been used to offline calculate the PRW variables according to Equations 2.1, 2.2, 2.3.
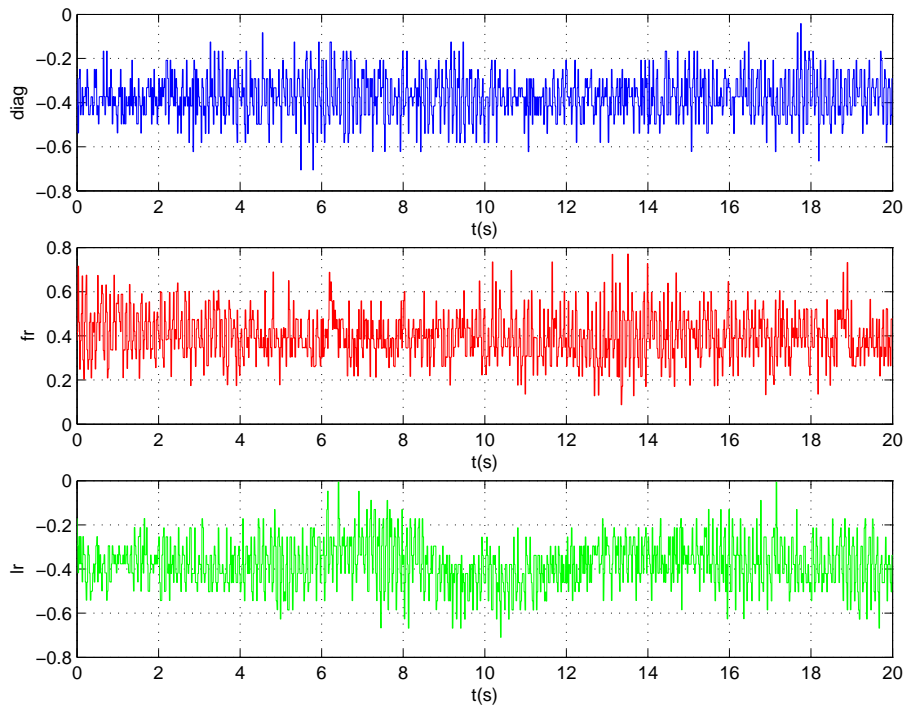


Figure 2.2: The PRW variables *diag* (top, blue), *fr* (middle, red) and *lr* (bottom, green) with one tyre, wheel 2 (FR), about 50% deflated.

## 2.2.2  Two tyres – equally deflated

If two tyres are deflated the outcome is immediately more uncertain. It is possible that the PRW does not react at all, depending on which two tyres that are deflated and by how much. For two equally deflated tyres to stand a chance of being detected they have to be located on the diagonal opposite of each other. Consider for example two equally deflated tyres located on the right side of the vehicle:

$$\left.\begin{array}{ll} \omega_1 & \rightarrow \\ \omega_2 & \uparrow \\ \omega_3 & \rightarrow \\ \omega_4 & \uparrow \end{array}\right\} \implies \left.\begin{array}{ll} diag & \rightarrow \\ fr & \rightarrow \\ lr & \downarrow \end{array}\right\} \Rightarrow \text{no warning}$$

The problem here is that the variable *diag* does not change. In reality it will fluctuate some due to noise from the wheel speed sensors but not enough to exceed the threshold value, see Figure 2.3. For this figure, the angular wheel speed data from a measurement with two tyres, the front right and the rear right, around 50% deflated have been evaluated offline using Equations 2.1, 2.2, 2.3. A similar situation arises for two equally deflated tyres on the left side, front or rear of the vehicle.
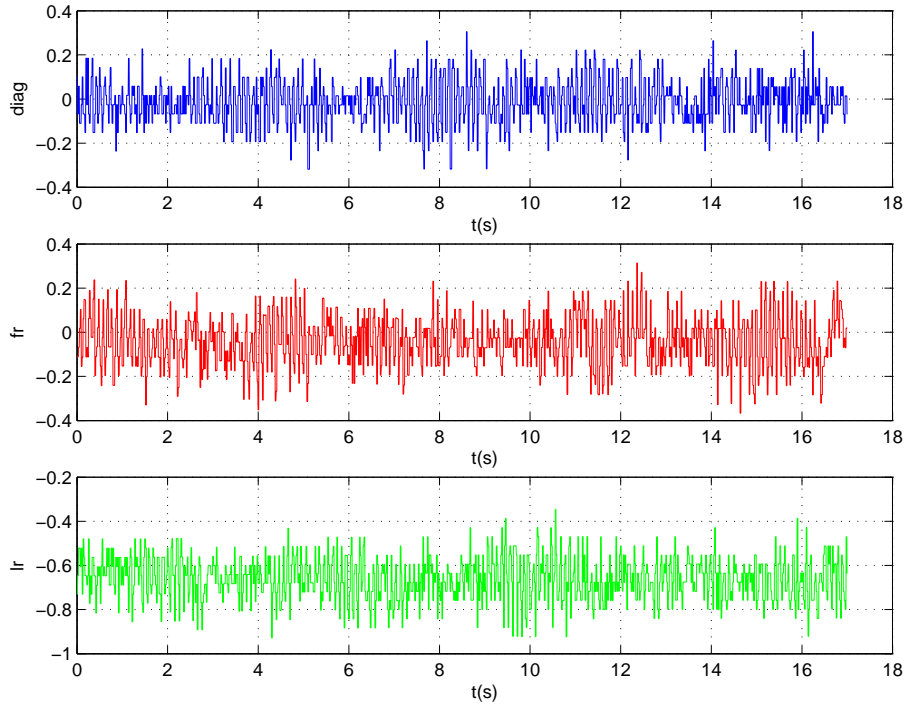


Figure 2.3: The PRW variables *diag* (top, blue), *fr* (middle, red) and *lr* (bottom, green) with the two tyres, wheel 2 (FR) and wheel 4 (RR), about 50% deflated.

### 2.2.3   Two tyres – not equally deflated

For two unequally deflated tyres the outcome again depends on which tyres that are deflated but also by how much in comparison to each other. For example, say the tyre on wheel 2 (FR) is 50% deflated and on wheel 4 (RR) is 75% deflated:

$$\left.\begin{array}{ll} \omega_1 & \rightarrow \\ \omega_2 & \uparrow \\ \omega_3 & \rightarrow \\ \omega_4 & \uparrow\uparrow \end{array}\right\} \implies \left.\begin{array}{ll} diag & \uparrow \\ fr & \downarrow \\ lr & \downarrow \end{array}\right\} \Rightarrow \text{RR warning}$$

In this case, since the tyre on wheel 4 (RR) is more deflated than the tyre on wheel 2 (FR) the *diag* variable will change and a detection is possible. This is of course only one simplified example, a complete analyse of the outcome is far more complicated. The amount of different combinations of selecting two tyres from four is six and by adding variants with different pressure levels, the number of possible scenarios that could arise become too many to go through in detail here. What is important to notice is that for two unequally deflated tyres it is possible that the PRW detects the deflation but it is not certain.

### 2.2.4 Three or four tyres deflated

For three or four deflated tyres the outcome again depends on how large the pressure difference is amongst the deflated tyres. Certain, however, is that four equally deflated tyres can not be detected.

## 2.3 Corrections

The following corrections are made in the PRW algorithm [3].

- **Offset correction.** Initial differences in angular wheel speed between the wheels, due to small variance in tyre pressure and possible difference in tyre size between front and rear tyres, are compensated for. These offsets will change with speed and therefore there are different offset values depending on how fast the vehicle moving.

- **Cornering correction.** When cornering, the angular wheel speeds will differ since the outer wheels travel a longer distance than the inner wheels. Also, there is a shift in weight from left to right or right to left, depending on the direction of turn, influencing the tyre dynamic radius for the non-drive axle and the tyre slip for the drive axle. This will also be compensated for in the PRW algorithm.

## 2.4 Rejections

For some conditions, the angular wheel speed signals are unsuitable for tyre deflation monitoring. These situations are recognized by the PRW and the signal data captured during this time is rejected, i.e. not used in any calculations. The different states are [3]:

- **Low speed.** At a very low speed, the angular wheel speed signals tend to contain too many errors and the signals should therefore not be used.

- **Strong longitudinal acceleration.** The angular wheel speed signals are error prone when the vehicle is undergoing heavy braking or strong acceleration.

- **Strong lateral acceleration.** The difference between outer and inner angular wheel speeds can trigger a false warning. This is normally compensated for with cornering correction, however this is not valid when the acceleration is too strong.

- **Extreme road conditions.** With the following road conditions the angular wheel speed data should be rejected:

  - Driving on a rough road.
  - Different road conditions between left and right wheel pair, that is, one side experiences higher slip than the other side, causes angular wheel speeds on the different sides to differ.
  - Road bank is too steep.

- **Extreme vehicle maneuver.** In the case of extreme driving the angular wheel speed data should be rejected.

## 2.5 Summary

This chapter was intended to give an insight to the main functionality of the PRW. The basic parts of the algorithm was presented and analysed for some different combinations of tyre pressure loss, with logical reasoning and offline evaluation of the PRW variables.

# Chapter 3

# PRW and warp

In this chapter the influences of warp on the PRW is discussed and investigated. Section 3.1 brings up important aspects of the problem which are then analysed in Section 3.2. The issue of different tyres is analysed in Section 3.3 and some concluding remarks are made in Section 3.4.

## 3.1 Influences from warp

Since warp changes wheel load, the tyre's dynamic radius is affected when driving with warp. The magnitude of the radius will deviate from its normal value depending on whether the wheel load has increased or decreased on that wheel. An increasing wheel load will cause the dynamic radius to decrease and vice versa. To analyse why driving with warp triggers false warnings and if it is possible to compensate for this in the PRW algorithm, it is important to establish:

- How the dynamic radius changes with tyre pressure.

- How the dynamic radius changes with wheel load (warp).

- How the variables *diag*, *fr* and *lr* change with tyre pressure.

- How the variables *diag*, *fr* and *lr* change with warp.

- For the all the above items: Is the behaviour velocity dependent?

- Is the behaviour independent of tyre make and dimensions?

### 3.1.1 Theoretical reasoning

Warp's influence on the PRW is similar to the case of two equally deflated tyres located on the diagonal to each other. The two wheels undergoing increased wheel load due to warp will react similar to the two deflated wheels, they will start to turn faster. The difference between these two cases is that warp affects all four wheels, there are two wheels that will experience less wheel load than normal and thus turn slower. In theory, positive warp will have the following effect on the wheel loads, dynamic radii, wheel speeds and PRW variables:

$$
\left.\begin{array}{ll} F_{z,1} & \uparrow \\ F_{z,2} & \downarrow \\ F_{z,3} & \downarrow \\ F_{z,4} & \uparrow \end{array}\right\} \Longrightarrow \left.\begin{array}{ll} rdyn_1 & \downarrow \\ rdyn_2 & \uparrow \\ rdyn_3 & \uparrow \\ rdyn_4 & \downarrow \end{array}\right\} \Longrightarrow \left.\begin{array}{ll} \omega_1 & \uparrow \\ \omega_2 & \downarrow \\ \omega_3 & \downarrow \\ \omega_4 & \uparrow \end{array}\right\} \Longrightarrow \begin{array}{ll} diag & \Uparrow \\ fr & \rightarrow \\ lr & \rightarrow \end{array}
$$

and negative warp

$$
\left.\begin{array}{ll} F_{z,1} & \downarrow \\ F_{z,2} & \uparrow \\ F_{z,3} & \uparrow \\ F_{z,4} & \downarrow \end{array}\right\} \Longrightarrow \left.\begin{array}{ll} rdyn_1 & \uparrow \\ rdyn_2 & \downarrow \\ rdyn_3 & \downarrow \\ rdyn_4 & \uparrow \end{array}\right\} \Longrightarrow \left.\begin{array}{ll} \omega_1 & \downarrow \\ \omega_2 & \uparrow \\ \omega_3 & \uparrow \\ \omega_4 & \downarrow \end{array}\right\} \Longrightarrow \begin{array}{ll} diag & \Downarrow \\ fr & \rightarrow \\ lr & \rightarrow \end{array}
$$

Hence, according to this reasoning, *diag* is the only variable affected by warp.

## 3.2 Test results

Warp's influence on dynamic radius can not be observed in any of the tyre models currently available. Thus, a number of measurements have been captured and analysed in order to establish the influence of warp compared to tyre pressure. The different situations, according to the list in the beginning of Section 3.1, are analysed below using the results from these measurements.

### 3.2.1 Measurements details

All measurements are captured driving on a test track. Since the PRW has some limits, as was shown in Section 2.2, only a pressure loss in one tyre can be detected for certain. Consequently, for parts where the influence of tyre pressure is analysed, only the case when one tyre undergoes pressure loss is investigated. All in all, the following situations are considered in this chapter:

- **Low pressure on one tyre without warp.** Driving straight ahead with decreased pressure on one tyre. Three different pressure levels are considered: 2.8 bar (normal), 2.1 bar and 1.5 bar.

- **Normal pressure on all tyres with warp.** Applying a sinusoid warp, see Figure 3.5, while driving at 60, 80 and 120 km/h. The turning force due to warp is compensated for by the driver such that the vehicle is kept in a straight line. All tyres have a normal pressure level (2.8 bar).

- **Different tyres.** Comparison between different tyre brands and dimensions is done in Section 3.3.

The angular wheel speed signals are taken from the ABS system. The velocity, which actually is an estimate of the average velocity of the vehicle since there is no signal available to measure the tangential velocity at each wheel, is derived from the wheel speeds. A reference velocity has also been used which was captured with an optical sensor, mounted on on the side of the vehicle. The errors introduced when using the average velocity of the vehicle instead of the tangential velocities are minor with the style of driving in these tests, no strong lateral acceleration or cornering, and can be neglected for the purpose of this investigation. The dynamic radius is calculated according to Equation 1.1.

### 3.2.2 Dynamic radius dependence on tyre pressure

First, it is desirable to establish how much the dynamic radius changes with tyre pressure. The dynamic radius is calculated with the angular wheel speeds and the average velocity of the vehicle. For these calculations, the reference velocity signal from the optical sensor has been used. Three velocities are considered – 60 km/h, 80 km/h and 120 km/h – as well as three different pressure levels:

- 2.8 bar – normal pressure

- 2.1 bar – 25% deflation

- 1.5 bar – almost 50% deflation
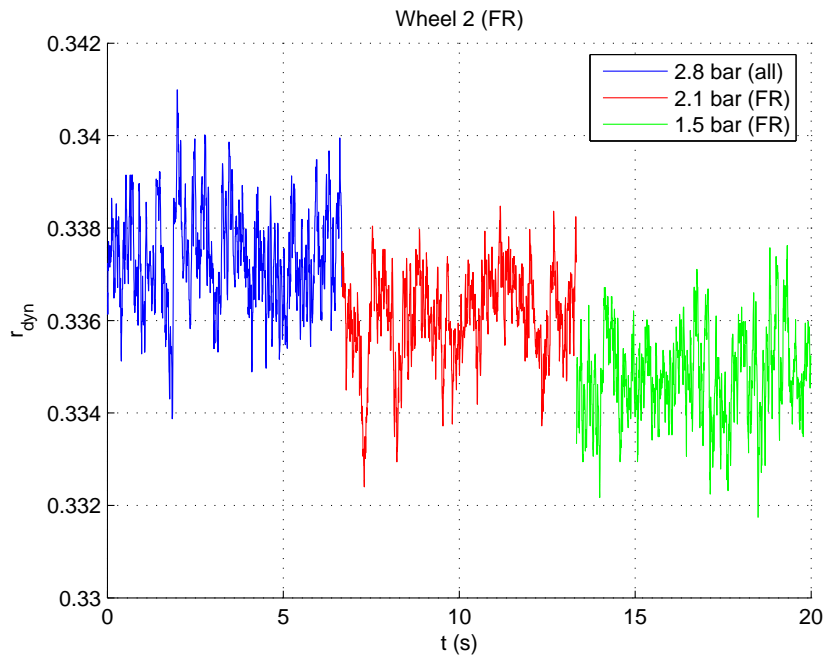


Figure 3.1: The dynamic radius of **wheel 2 (FR)** for three different pressure levels at 80 km/h. For the first sequence (blue) all tyres are correctly inflated (2.8 bar), for the second sequence (red) wheel 2 (FR) has a pressure of 2.1 bar whilst the others remain unchanged and for the third sequence (green) wheel 2 (FR) is further deflated to a pressure of 1.5 bar.

The calculated dynamic radius of wheel 2 (FR), the wheel with the deflated tyre, can be seen in Figure 3.1, wheel 1 (FL) in Figure 3.2, wheel 3 (RL) in Figure 3.3 and wheel 4 (RR) in Figure 3.4. In the figures, the result from three different measurements with different pressure levels have been plotted together. The velocity was 80 km/h. The first part (blue) shows the result from having all tyres correctly inflated. For the second part (red) the front right tyre is deflated to a pressure of 2.1 bar and for the third part (green) the front right tyre is further deflated to a pressure of 1.5 bar. As expected, the front right tyre shows a decrease in dynamic radius with lower pressure whilst the other remain unchanged.
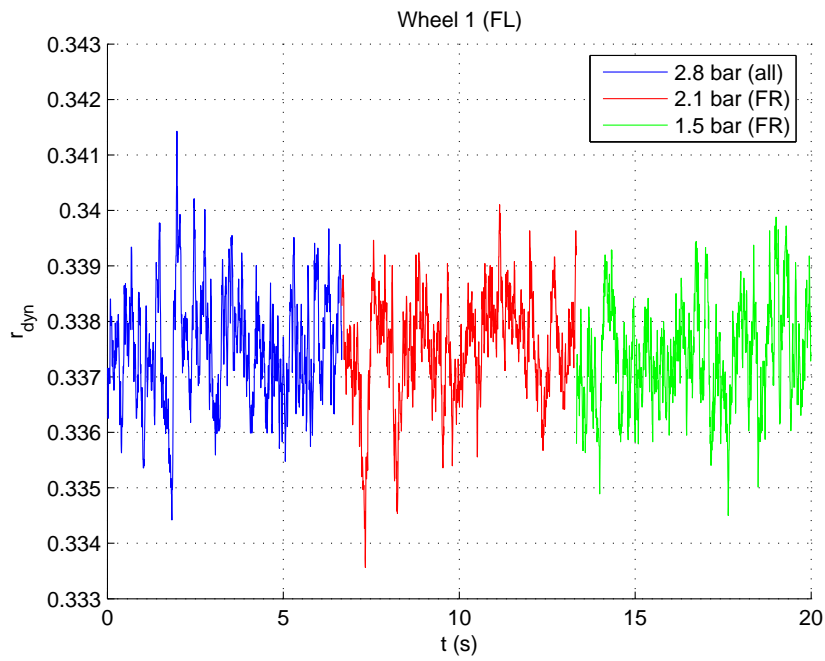
Figure 3.2: The dynamic radius of **wheel 1 (FL)** for three different pressure levels at 80 km/h. For the first sequence (blue) all tyres are correctly inflated (2.8 bar), for the second sequence (red) wheel 2 (FR) has a pressure of 2.1 bar whilst the others remain unchanged and for the third sequence (green) wheel 2 (FR) is further deflated to a pressure of 1.5 bar.
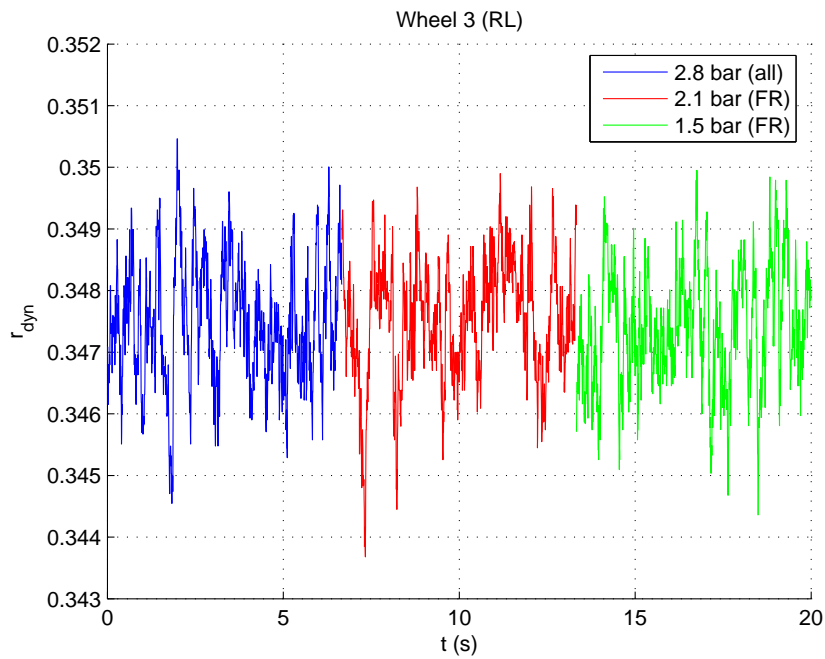
Figure 3.3: The dynamic radius of **wheel 3 (RL)** for three different pressure levels at 80 km/h. For the first sequence (blue) all tyres are correctly inflated (2.8 bar), for the second sequence (red) wheel 2 (FR) has a pressure of 2.1 bar whilst the others remain unchanged and for the third sequence (green) wheel 2 (FR) is further deflated to a pressure of 1.5 bar.
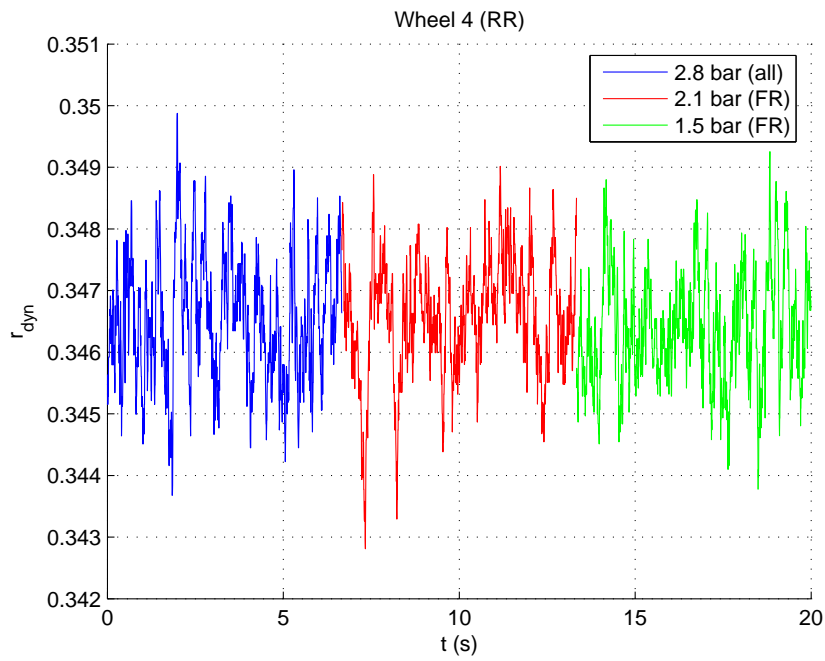
Figure 3.4: The dynamic radius of **wheel 4 (RR)** for three different pressure levels at 80 km/h. For the first sequence (blue) all tyres are correctly inflated (2.8 bar), for the second sequence (red) wheel 2 (FR) has a pressure of 2.1 bar whilst the others remain unchanged and for the third sequence (green) wheel 2 (FR) is further deflated to a pressure of 1.5 bar.

Mean values from several measurements with different velocities and pressures, from the same test track, can be seen in Table 3.1 (60 km/h), Table 3.2 (80 km/h) and Table 3.3 (120 km/h). The results show that a deflation of about 50% results in a change in dynamic radius of around 0.0025 m, for these tyres.

Table 3.1: Mean values of the calculated dynamic radius (m) for all tyres at a velocity of **60 km/h**. First column with 2.8 bar, normal pressure on all tyres, second column with 2.1 bar on wheel 2 (FR) and third column with 1.5 bar on wheel 2 (FR).

| 60 km/h | 2.8 bar (all) | 2.1 bar (FR) | 1.5 bar (FR) | $\Delta_{2.8-2.1}$ | $\Delta_{2.8-1.5}$ |
|---|---|---|---|---|---|
| wheel 1 (FL) | 0.3369 | 0.3371 | 0.3371 | - | - |
| wheel 2 (FR) | 0.3367 | 0.3357 | 0.3345 | -0.001 | -0.0022 |
| wheel 3 (RL) | 0.3470 | 0.3472 | 0.3471 | - | - |
| wheel 4 (RR) | 0.3460 | 0.3462 | 0.3461 | - | - |

Table 3.2: Mean values of the calculated dynamic radius (m) for all tyres at a velocity of **80 km/h**. First column with 2.8 bar, normal pressure on all tyres, second column with 2.1 bar on wheel 2 (FR) and third column with 1.5 bar on wheel 2 (FR).

| 80 km/h | 2.8 bar (all) | 2.1 bar (FR) | 1.5 bar (FR) | $\Delta_{2.8-2.1}$ | $\Delta_{2.8-1.5}$ |
|---|---|---|---|---|---|
| wheel 1 (FL) | 0.3378 | 0.3376 | 0.3376 | - | - |
| wheel 2 (FR) | 0.3377 | 0.3362 | 0.3349 | -0.0015 | -0.0028 |
| wheel 3 (RL) | 0.3478 | 0.3477 | 0.3476 | - | - |
| wheel 4 (RR) | 0.3469 | 0.3466 | 0.3466 | - | - |

Table 3.3: Mean values of the calculated dynamic radius (m) for all tyres at a velocity of **120 km/h**. First column with 2.8 bar, normal pressure on all tyres, second column with 2.1 bar on wheel 2 (FR) and third column with 1.5 bar on wheel 2 (FR).

| 120 km/h | 2.8 bar (all) | 2.1 bar (FR,RR) | 1.5 bar (FR,RR) | $\Delta_{2.8-2.1}$ | $\Delta_{2.8-1.5}$ |
|---|---|---|---|---|---|
| wheel 1 (FL) | 0.3367 | 0.3367 | 0.3366 | - | - |
| wheel 2 (FR) | 0.3366 | 0.3352 | 0.3340 | -0.0014 | -0.0026 |
| wheel 3 (RL) | 0.3466 | 0.3466 | 0.3465 | - | - |
| wheel 4 (RR) | 0.3457 | 0.3456 | 0.3455 | - | - |

### 3.2.3 Dynamic radius as a function of wheel load

A sinusoid warp input with an amplitude of around max warp force, see Figure 3.5, gives a good overview of how the dynamic radius changes with wheel load. With a sinusoid warp input the whole spectrum from minimum to maximum warp level is accounted for. The dynamic
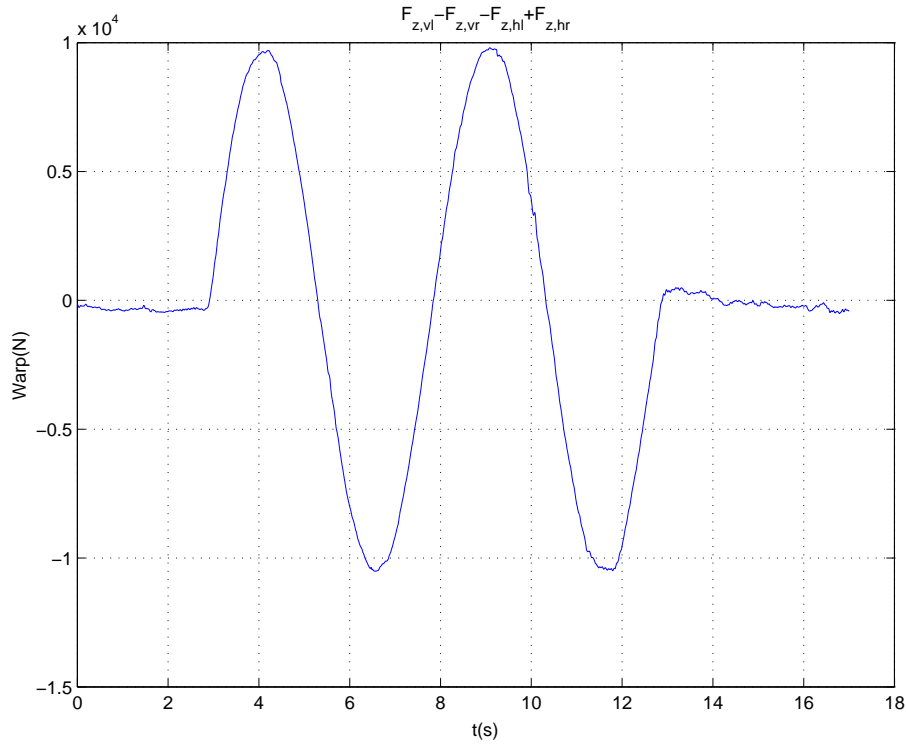
Figure 3.5: Sinusoid warp, 10 kN

radius is calculated from measurements with three different velocities. The result from 60 km/h can be seen in Figure 3.6, 80 km/h in Figure 3.7 and 120 km/h in Figure 3.8.

From these figures, the following can be established:

- The behaviour is different for front and rear tyres.

- For the front wheels, with these wheel loads, the relationship is almost linear.

- For the rear wheels, the relationship at negative and positive wheel loads can be approximated with linear functions with different gradients. This is most likely due to the difference in width between the front and the rear tyres. The rear tyres have a width of 275 mm and the width of the front tyres are 255 mm.

- The change in dynamic radius is at most around 1.25 mm, on average, for the front wheels and for the rear wheels with positive wheel load. For negative wheel load at the rear wheels the change is on average at most around 0.7 mm.

Even though the results derived in this section suggest that the relationship between wheel load and dynamic radius is linear, this is not the case for all possible values of wheel load. Consider, for example, the two extreme cases no wheel load and maximum wheel load, which could be the maximum allowed load for the particular tyre. For both cases the dynamic radius will reach a limit value and moving towards this limit the rate of change in radius is likely to decrease. The general idea of the complete function can be seen in Figure 3.9. The figure also points out the area of the curve which applies to having normal wheel load with minimum or

18
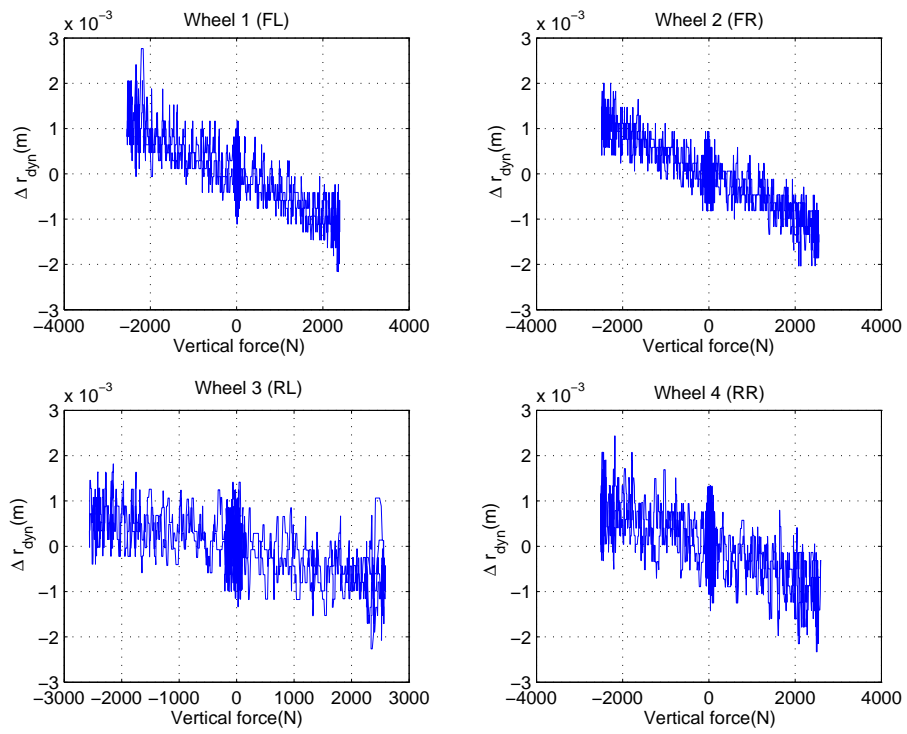
Figure 3.6: Change in dynamic radius as a function of wheel load – 60 km/h
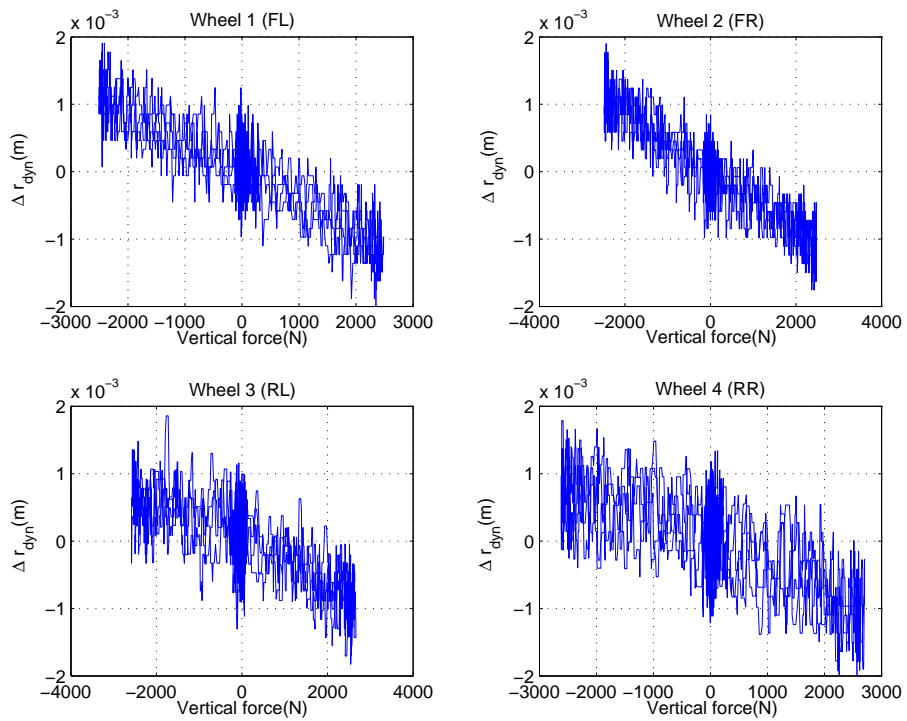


Figure 3.7: Change in dynamic radius as a function of wheel load – 80 km/h
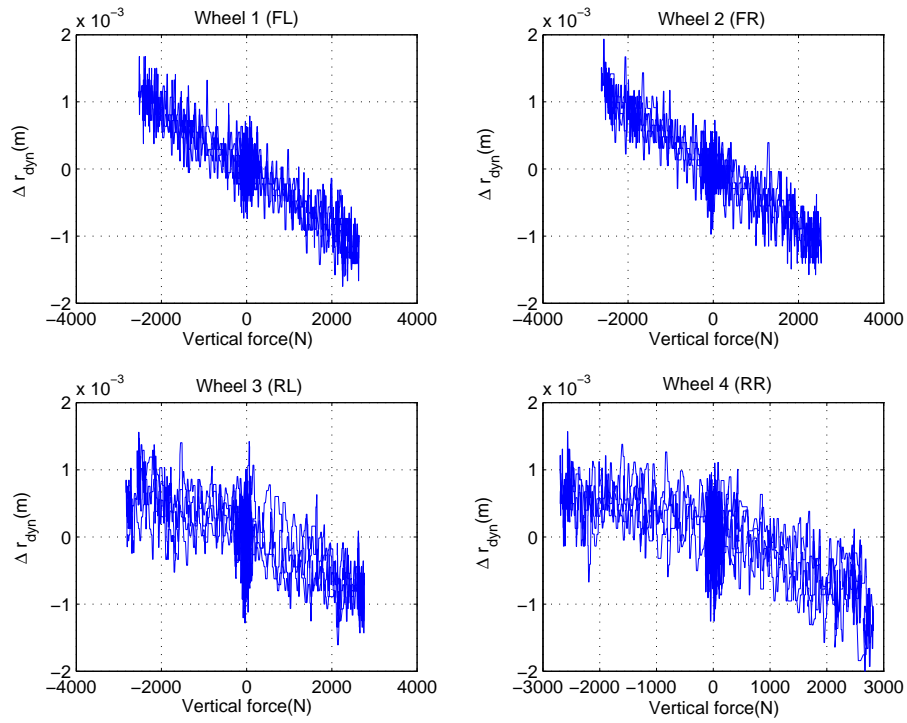
Figure 3.8: Change in dynamic radius as a function of wheel load – 120 km/h
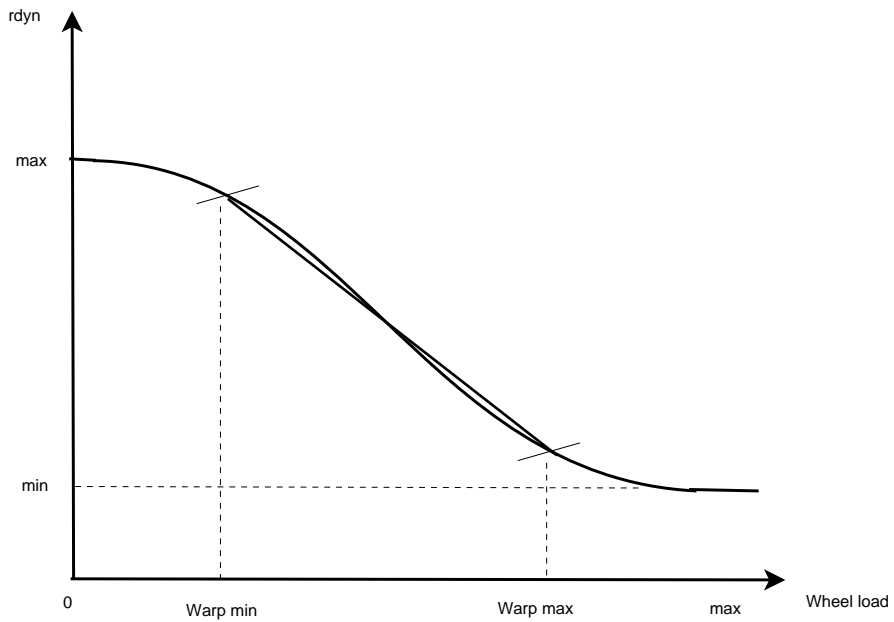


Figure 3.9: Estimated function for the relationship between dynamic radius and wheel load.

maximum warp. This explains why the relationship between wheel load and dynamic radius appears to be fairly linear in the previously presented plots derived from field measurements.

To see if a velocity dependent behaviour can be found, a linear approximation is made for the two front wheels for all three measurements shown in these figures. The result can be seen in Table 3.4.

Table 3.4: Linear approximation of $r_{dyn}$ over wheel load for the front wheels

| $\Delta r_{dyn} = p1 \cdot F_i + p2$ | $p1$ | $p2$ | $norm\ of\ residuals$ |
|---|---|---|---|
| 60 (FL) | $-4.6549 \cdot 10^{-7}$ | $1.7666 \cdot 10^{-15}$ | 0.0178 |
| 60 (FR) | $-4.6137 \cdot 10^{-7}$ | $-1.8432 \cdot 10^{-15}$ | 0.0159 |
| 80 (FL) | $-4.4013 \cdot 10^{-7}$ | $1.1866 \cdot 10^{-15}$ | 0.0172 |
| 80 (FR) | $-4.4060 \cdot 10^{-7}$ | $1.8949 \cdot 10^{-15}$ | 0.0180 |
| 120 (FL) | $-4.4103 \cdot 10^{-7}$ | $-1.0596 \cdot 10^{-15}$ | 0.0117 |
| 120 (FR) | $-4.3598 \cdot 10^{-7}$ | $-1.7245 \cdot 10^{-15}$ | 0.0114 |

The linear approximation suggests that there is a trend towards a less steep gradient with higher velocities. Thus, the dynamic radius is more affected by warp at lower velocities than at higher. There is, for this particular tyre, however only a small difference, comparing $\Delta r_{dyn}$ for the front right tyre at 60 km/h and 120 km/h at a wheel load of -2500 N (neglecting the $p2$ value) gives:

$$\begin{aligned} \Delta r_{dyn}^{60} &= (-4.6137) \cdot 10^{-7} \cdot (-2500) \approx 0.0012 \\ \Delta r_{dyn}^{120} &= (-4.3598) \cdot 10^{-7} \cdot (-2500) \approx 0.0011 \end{aligned}$$

The difference is thus only 0.0001 m, around 8%. Hence, the influence from velocity seems to be small.

### 3.2.4   Change in PRW variables due to low tyre pressure

The PRW variables *diag*, *fr* and *lr* are calculated according to Equation 2.1, Equation 2.2 and Equation 2.3, respectively, with wheel speed data from measurements with three different tyre pressure levels:

- 2.8 bar – normal pressure

- 2.1 bar – 25% deflation

- 1.5 bar – almost 50% deflation

The *diag* variable can be seen in Figure 3.10, the variable *fr* in Figure 3.11 and the variable *lr* in Figure 3.12. The velocity was 80 km/h for all of them. Further, to see possible discrepancies between different velocities and tyre pressures, the mean values of the PRW variables from several measurements with three different velocities and tyre pressures are derived. The result can be seen in Table 3.5 for 60 km/h, Table 3.6 for 80 km/h and Table 3.7 for 120 km/h. In all plots, the corresponding offset for the particular variable at 80 km/h has
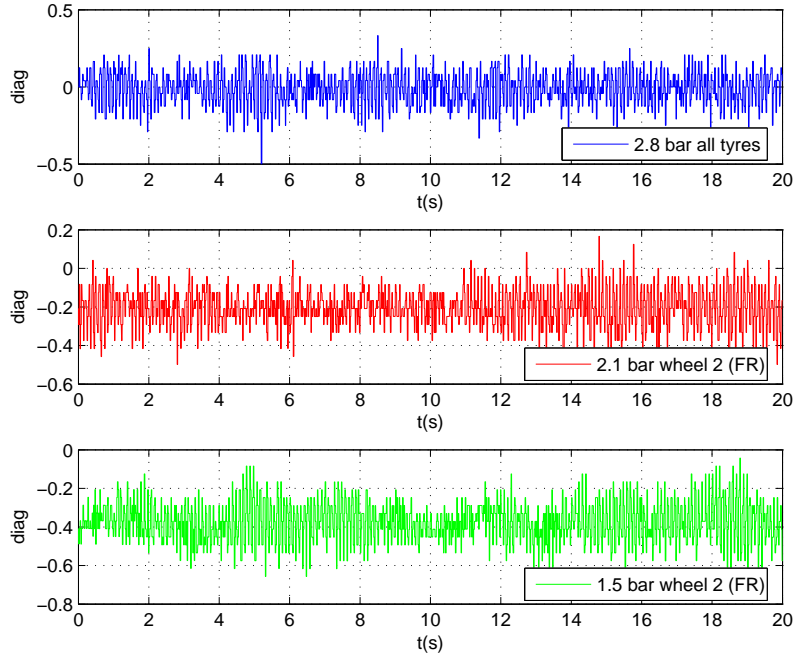
Figure 3.10: The variable *diag* for three different tyre pressures. Offset has been deducted. Top figure (blue) for 2.8 bar on all tyres, middle figure (red) for 2.1 bar on wheel 2 (FR) and bottom figure (green) for 1.5 bar on wheel 2 (FR). Velocity was 80 km/h.

Table 3.5: Mean values of the PRW variables *diag*, *fr* and *lr* for three different pressures: 2.8 bar on all tyres, 2.1 bar on wheel 2 (FR) and 1.5 bar on wheel 2 (FR) – **60 km/h**. Offset has not been deducted.

| 60 km/h | 2.8 bar | 2.1 bar (FR) | 1.5 bar (FR) | $\Delta_{2.8-2.1}$ | $\Delta_{2.8-1.5}$ |
|---------|---------|--------------|--------------|---------|---------|
| *diag* | 0.1208 | -0.0709 | -0.2542 | -0.1917 | -0.3750 |
| *fr* | 2.8606 | 3.0634 | 3.2374 | 0.2028 | 0.3768 |
| *lr* | -0.1470 | -0.3705 | -0.5371 | -0.2235 | -0.3901 |

Table 3.6: Mean values of the PRW variables *diag*, *fr* and *lr* for three different pressures: 2.8 bar on all tyres, 2.1 on wheel 2 (FR) and 1.5 bar on wheel 2 (FR) – **80 km/h**. Offset has not been deducted.

| 80 km/h | 2.8 bar | 2.1 bar | 1.5 bar | $\Delta_{2.8-2.1}$ | $\Delta_{2.8-1.5}$ |
|---------|---------|---------|---------|---------|---------|
| *diag* | 0.1200 | -0.0791 | -0.2480 | -0.1991 | -0.3680 |
| *fr* | 2.8395 | 3.0441 | 3.2277 | 0.2046 | 0.3882 |
| *lr* | -0.1539 | -0.3650 | -0.5384 | -0.2111 | -0.3845 |
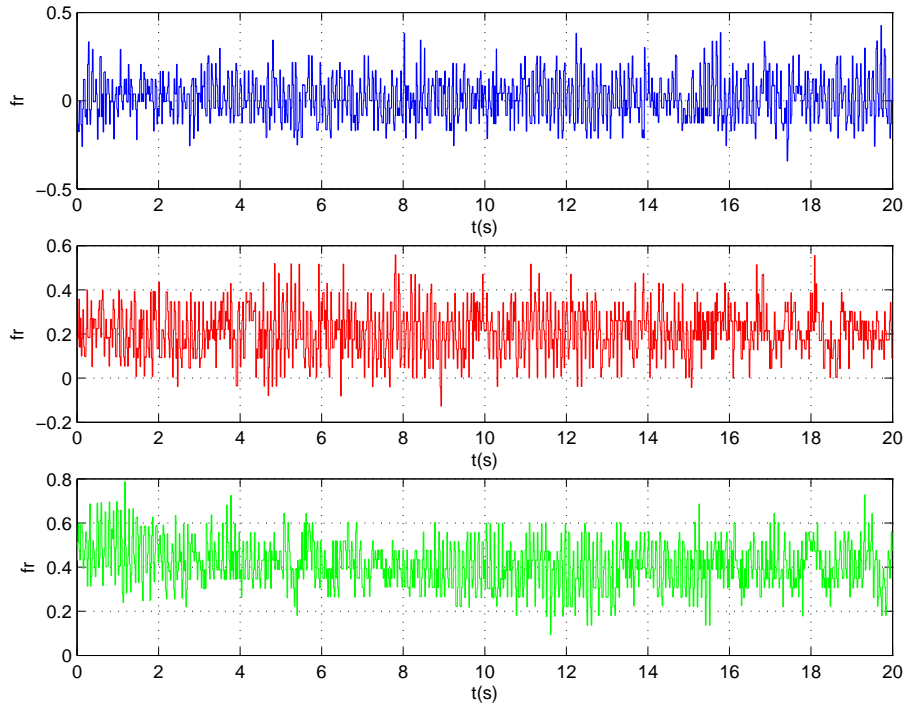
Figure 3.11: The variable *fr* for three different tyre pressures. Offset has been deducted. Top figure (blue) for 2.8 bar on all tyres, middle figure (red) for 2.1 bar on wheel 2 (FR) and bottom figure (green) for 1.5 bar on wheel 2 (FR). Velocity was 80 km/h.

Table 3.7: Mean values of the variables *diag*, *fr* and *lr* for three different pressures: 2.8 bar on all tyres, 2.1 bar on wheel 2 (FR) and 1.5 bar on wheel 2 (FR) – **120 km/h**. Offset has not been deducted.

| **120 km/h** | 2.8 bar | 2.1 bar | 1.5 bar | $\Delta_{2.8-2.1}$ | $\Delta_{2.8-1.5}$ |
|---|---|---|---|---|---|
| *diag* | 0.1209 | -0.0733 | -0.2449 | -0.1942 | -0.3658 |
| *fr* | 2.8130 | 3.0290 | 3.1927 | 0.2160 | 0.3797 |
| *lr* | -0.1608 | -0.3669 | -0.5367 | -0.2061 | -0.3759 |
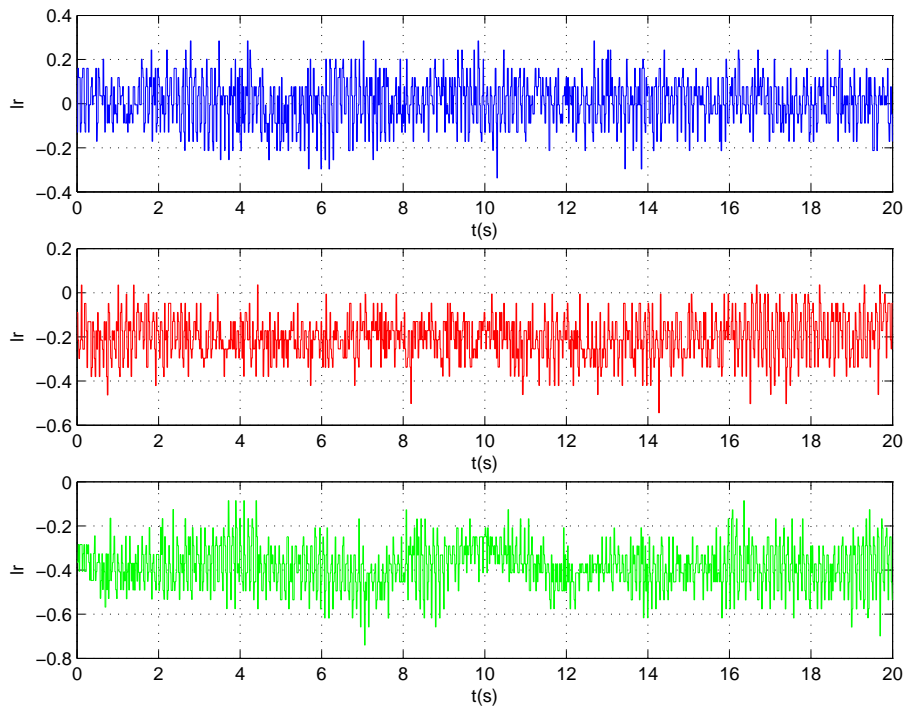
Figure 3.12: The variable *lr* for three different tyre pressures. Offset has been deducted. Top figure (blue) for 2.8 bar on all tyres, middle figure (red) for 2.1 bar on wheel 2 (FR) and bottom figure (green) for 1.5 bar on wheel 2 (FR). Velocity was 80 km/h.

been deducted. For the mean value calculations seen in the tables, however, this is not done. Only the change in value is of interest and not the value itself.

When capturing the measurements used in this section, it is the front right tyre that has been deflated. This can be verified by comparing the results to the PRW warning table, see Table 2.1, where a negative *diag* value, a positive *fr* value and a negative *lr* value results in a *FR* warning. When looking at the results showing the influence from velocity, it can be concluded that a higher velocity results in a smaller influence by tyre pressure for all PRW variables. There is only one exception, the value of the *fr* variable at 60 km/h is smaller than the value of the same variable at 80 km/h.

### 3.2.5  Change in PRW variables due to warp

As the *diag* variable is crucial for the tyre deflation warning it is necessary to observe how much it changes with warp. The *fr* and *lr* variables are also of interest, even though, according to the theoretical reasoning earlier, these should not be affected by warp.
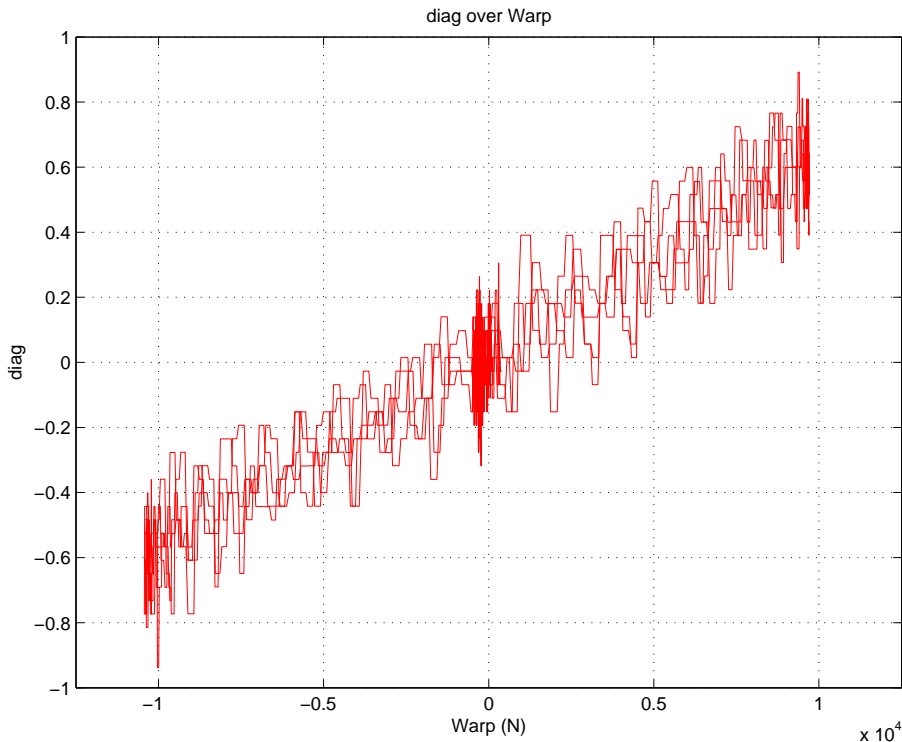


Figure 3.13: *diag* variable as a function of warp – 80 km/h

The three PRW variables are plotted as a function of warp. The variable *diag* can be seen in Figure 3.13, the variable *fr* in Figure 3.14 and the variable *lr* in Figure 3.15. The velocity for all measurements was 80 km/h. As predicted, the *diag* variable increases with positive warp and decreases with negative warp. The *fr* and *lr* variables, however, are not unaffected by warp which contradicts what was established in the theoretical discussion, in Section 3.1.1. The *fr* variable seems to take, on average, more negative than positive values for both positive and negative warp. The *lr* variable follows the same behaviour as the *diag* value – increases with positive warp and decreases with negative warp, although not as much

25
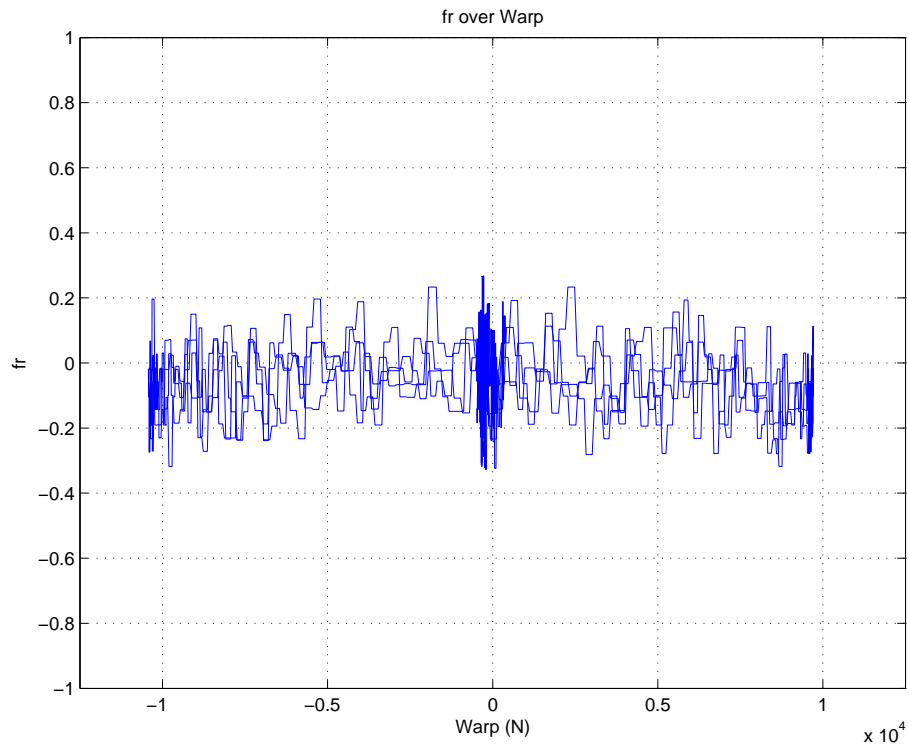
Figure 3.14: *fr* variable as a function of warp – 80 km/h
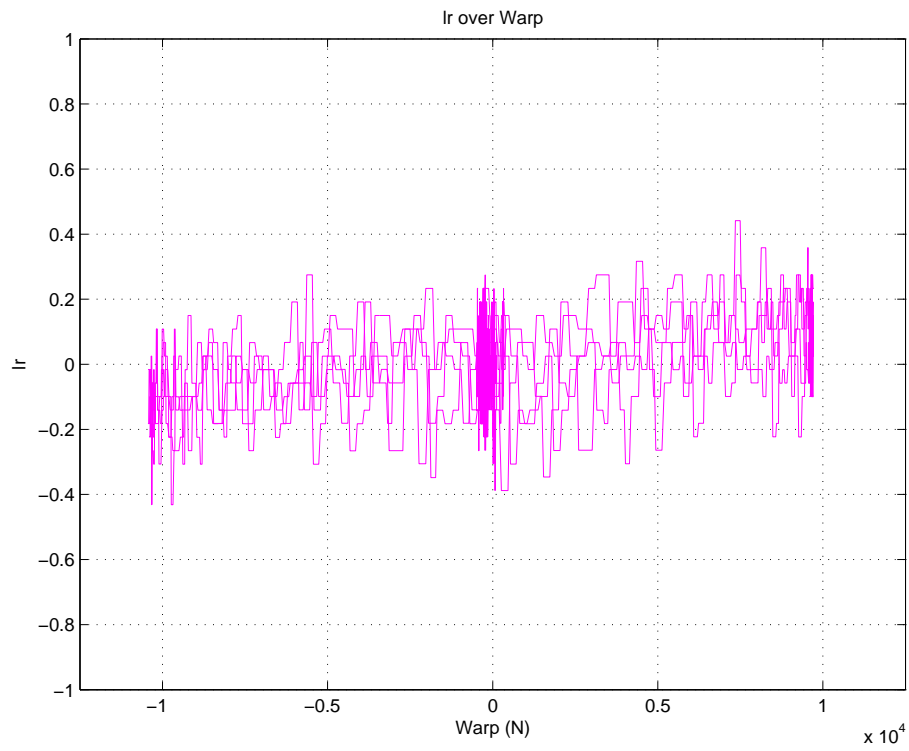


Figure 3.15: *lr* variable as a function of warp – 80 km/h

as *diag*. An explanation for this can be found by looking at the results from the dynamic radius over wheel load, see for example Figure 3.7. From these results, it was established that the change in dynamic radius was less for negative warp on the rear tyres than for all the other cases. The explanation for the different behaviour between the front and the rear tyres is that the rear tyres are wider than the front tyres. The effect on *diag*, *fr* and *lr* is thus with positive warp:

$$
\left.\begin{array}{ll}
\Delta rdyn_1 & -1 \\
\Delta rdyn_2 & +1 \\
\Delta rdyn_3 & +\frac{1}{2} \\
\Delta rdyn_4 & -1
\end{array}\right\} \Longrightarrow
\left.\begin{array}{ll}
\Delta\omega_1 & +1 \\
\Delta\omega_2 & -1 \\
\Delta\omega_3 & -\frac{1}{2} \\
\Delta\omega_4 & +1
\end{array}\right\} \Longrightarrow
\left.\begin{array}{ll}
diag & \frac{(\omega_1+\omega_4)\uparrow}{(\omega_2+\omega_3)\downarrow} \\[2mm]
fr & \frac{(\omega_1+\omega_2)\rightarrow}{(\omega_3+\omega_4)\uparrow} \\[2mm]
lr & \frac{(\omega_1+\omega_3)\uparrow}{(\omega_2+\omega_4)\rightarrow}
\end{array}\right\} \Longrightarrow
\left.\begin{array}{ll}
diag & \uparrow \\
fr & \downarrow \\
lr & \uparrow
\end{array}\right.
$$

and with negative warp

$$
\left.\begin{array}{ll}
\Delta rdyn_1 & +1 \\
\Delta rdyn_2 & -1 \\
\Delta rdyn_3 & -1 \\
\Delta rdyn_4 & +\frac{1}{2}
\end{array}\right\} \Longrightarrow
\left.\begin{array}{ll}
\Delta\omega_1 & -1 \\
\Delta\omega_2 & +1 \\
\Delta\omega_3 & +1 \\
\Delta\omega_4 & -\frac{1}{2}
\end{array}\right\} \Longrightarrow
\left.\begin{array}{ll}
diag & \frac{(\omega_1+\omega_4)\downarrow}{(\omega_2+\omega_3)\uparrow} \\[2mm]
fr & \frac{(\omega_1+\omega_2)\rightarrow}{(\omega_3+\omega_4)\uparrow} \\[2mm]
lr & \frac{(\omega_1+\omega_3)\rightarrow}{(\omega_2+\omega_4)\uparrow}
\end{array}\right\} \Longrightarrow
\left.\begin{array}{ll}
diag & \downarrow \\
fr & \downarrow \\
lr & \downarrow
\end{array}\right.
$$

A linear function approximation is done for *diag* as a function of warp. Several measurements from the same test track for each velocity have been collected for this purpose and the mean results can be seen in Table 3.8. The measurements show that *diag* is more affected by warp at the lower velocities than at the higher.

Table 3.8: The mean gradient for the three different velocities 60, 80 and 120 km/h as a result of the linear approximation of *diag* as a function of warp from five different measurements.

| *velocity (km/h)* | *mean gradient* |
|:---:|:---:|
| **60** | $6.126 \cdot 10^{-5}$ |
| **80** | $5.964 \cdot 10^{-5}$ |
| **120** | $5.606 \cdot 10^{-5}$ |

## 3.3 Different types of tyres

Important for this thesis is to investigate how much the tyre deforms under the influence of wheel load. The relationship between tyre deflection and wheel load is referred to as the *vertical stiffness* of the tyre. The tyre deflection is related to the dynamic radius as [4]:

$$r_{dyn} = r_0 - \frac{tyredefl}{3} \tag{3.1}$$

where $r_{dyn}$ is the dynamic radius and $r_0$ is the undeformed tyre radius at the same pressure level.

In the previous chapter, the change in dynamic radius due to wheel load was derived from measurements with the tyres Conti Sport Contact 2 with the dimensions 255/40 R19 96Y for the front tyres and 275/40 R19 101Y for the rear tyres. It is, however, likely that tyres with other dimensions and/or make will have other vertical stiffness curves, meaning that the change in dynamic radius due to wheel load, and therefore the influence by warp, will be different for different tyres. Also, even though the same tyres with the same dimensions are used, it is possible to have different initial pressure levels. For example, in the measurements in the previous section the 'normal' pressure level was set to 2.8 bar but a perfectly valid level would also have been 3.0 bar or 2.6 bar. The amount of pressure in the tyre is known to affect the vertical stiffness, the question is only by how much.

A load-deflection plot, giving a vertical stiffness curve, will be investigated for some different tyres, covering the following cases:

- Same tyre make and dimensions with different pressure levels.

- Different tyre make with same dimensions.

- Different dimensions with the same tyre make.

- Different tyre make and dimensions.

Measurements from the Karlsruhe University will be used, where a test environment for tyres is available. Most of the measurements have been captured in an internal drum test device, some with a velocity and some at a stand still.

### 3.3.1 Tyre dimensions

The numbers and letters associated with a tyre describe the characteristics and dimensions of the tyre. Taking the Conti 255/40 R19 96 Y as an example the different numbers implies:

- **255** Tyre width in millimetres.

- **40** Aspect ratio, the height of the side of the tyre expressed as a percentage of the width.

- **R** Stands for radial which means that the tyre is a radial constructed tyre.

- **19** Tyre rim size in inches.

- **96** Index for the maximum load that the tyre may be exposed to.

- **Y** Index for maximum recommended speed.

### 3.3.2 Different pressure levels

When new tyres have been fitted the driver must, after desired tyre pressure has been set, reinitialise the PRW such that the new pressure level will be recognized as the 'normal' pressure level. Thus, the driver has the possibility to, dependent on driving style and comfort preferences, choose different normal pressure levels. Of course, the choices of normal pressure level is restricted to what is recommended by the tyre brand and how heavy the vehicle is [6].

The load-deflection relationship for two Continental tyres have been plotted, Conti Sport Contact 2 with the dimensions 255/40 R19 96Y in Figure 3.16 and Continental 205/55 R16
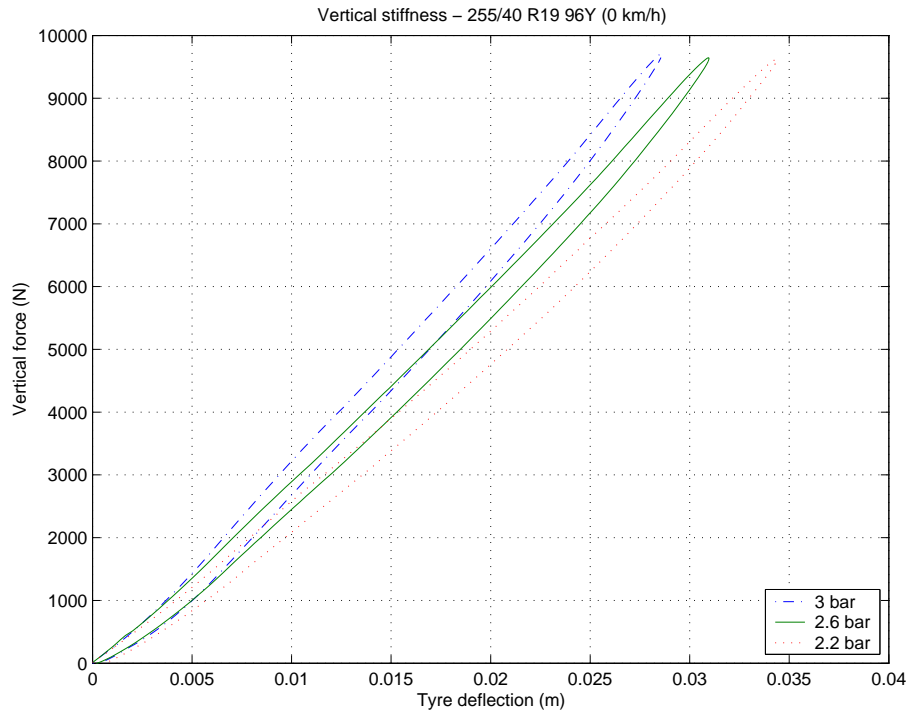
Figure 3.16: Load-deflection relationship for Continental 255/40 R19 at 3 bar, 2.6 bar and 2.2 bar, the velocity is 0 km/h.
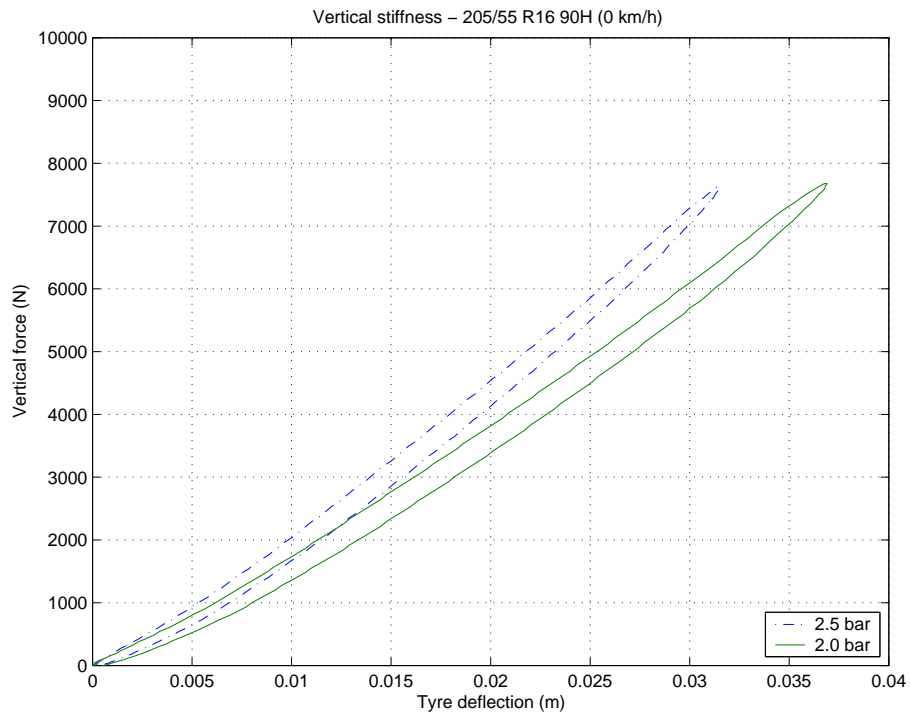


Figure 3.17: Load-deflection relationship for Continental 205/35 R16 at 2.5 bar and 2.0 bar, the velocity is 0 km/h.

90H in Figure 3.17. For both tyres the measurements were taken at a stand still. From the figures, it is clear that the vertical stiffness changes with pressure level. For the 205/55 R16 tyre the difference in tyre deflection at 6000 N is almost 17% between 2.5 bar and 2.0 bar. For the 255/40 R19 tyre the difference in tyre deflection between 3 bar and 2.6 bar at 8000 N is about 8%, between 2.6 bar and 2.2 bar around 10% and between 3 bar and 2.2 bar almost 18%.

### 3.3.3  Different make

To investigate how much different tyre brands could differ in terms of vertical stiffness, one Dunlop SP and one Bridgestone Potenza tyre have been compared. They both have the dimensions 225/35 R18, however the Dunlop tyre had a pressure of 2.5 bar and the Bridgestone tyre had a pressure of 2.2 bar. The result can be seen in Figure 3.18, the velocity was here 40 km/h.
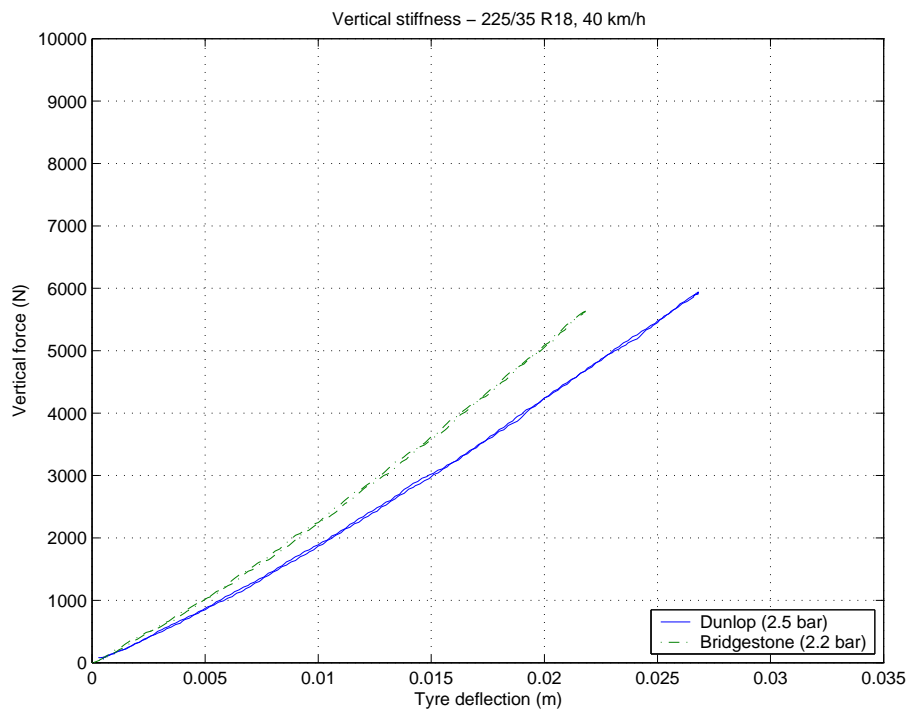


Figure 3.18: Load-deflection relationship for one Dunlop SP tyre and one Bridgestone Potenza tyre, both with the dimensions 225/35 R18, velocity 40 km/h.

It is interesting to notice, that even though the Bridgestone tyre had a pressure 0.3 bar lower than the Dunlop tyre, the Bridgestone tyre still deflects less with wheel load than the Dunlop tyre. This indicates that the make of the tyre does have an influence on the vertical stiffness, since according to the results just shown on how vertical stiffness increases with tyre pressure, the Bridgestone tyre should deflect more than the Dunlop tyre, considering they have the same dimensions. This is however not the case and it can therefore be concluded that the make of the tyre does affect vertical stiffness.

For example, at 4000 N the difference between the Dunlop tyre and the Bridgestone tyre is about 17%.

### 3.3.4   Different dimensions

Two Conti Eco Contact tyres have been compared to see the influence of different widths and aspect ratios on vertical stiffness. One tyre has the dimensions 225/60 R16 and the other 215/55 R16, thus they both have the same rim size. The result can be seen in Figure 3.19, the velocity was 80 km/h. At 4000 N, the tyre with the dimensions 215/55 R16 deflects about 3% more than the larger tyre. Thus, a tyre with smaller width and aspect ratio will have a slightly lower vertical stiffness than a larger tyre.
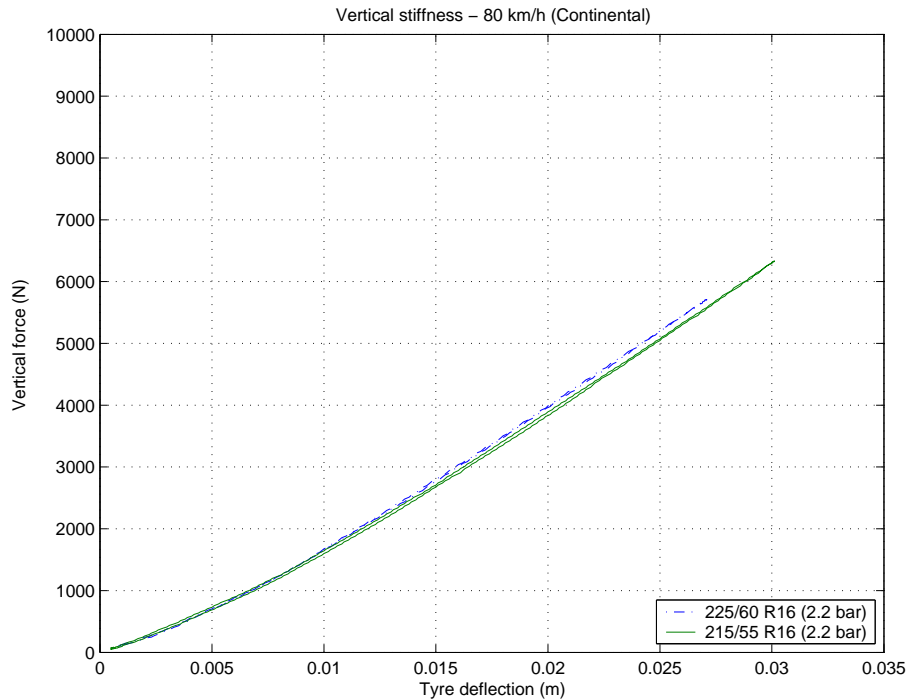


Figure 3.19: Load-deflection relationship for two Conti Eco Contact tyres, one with the dimensions 225/60 R16 and one with 215/55 R16, velocity 80 km/h.

### 3.3.5   Different make and different dimensions

Finally, two tyres with different dimensions and different make are compared. One Michelin Pilot Sport tyre with the dimensions 245/45 R18 and one Conti Sport Contact 2 with the dimensions 255/50 R19, both tyres have a pressure of 3 bar. The vertical stiffness curve for a velocity of 50 km/h can be seen in Figure 3.20 and for 100 km/h in Figure 3.21. The Michelin tyre clearly deflects more due to wheel load than the Conti tyre, at both 5000 N and 8000 N the difference is about 12.5%.
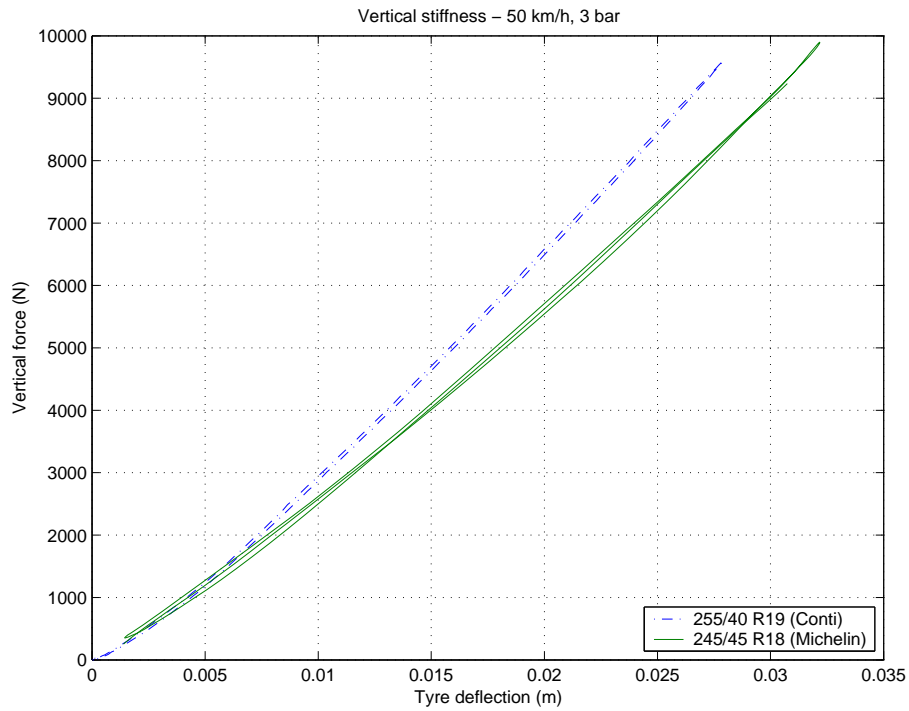
Figure 3.20: Load-deflection relationship for one Michelin Pilot Sport tyre with the dimensions 245/45 R18 and one Conti Sport Contact 2 with the dimensions 255/50 R19 - 50 km/h.
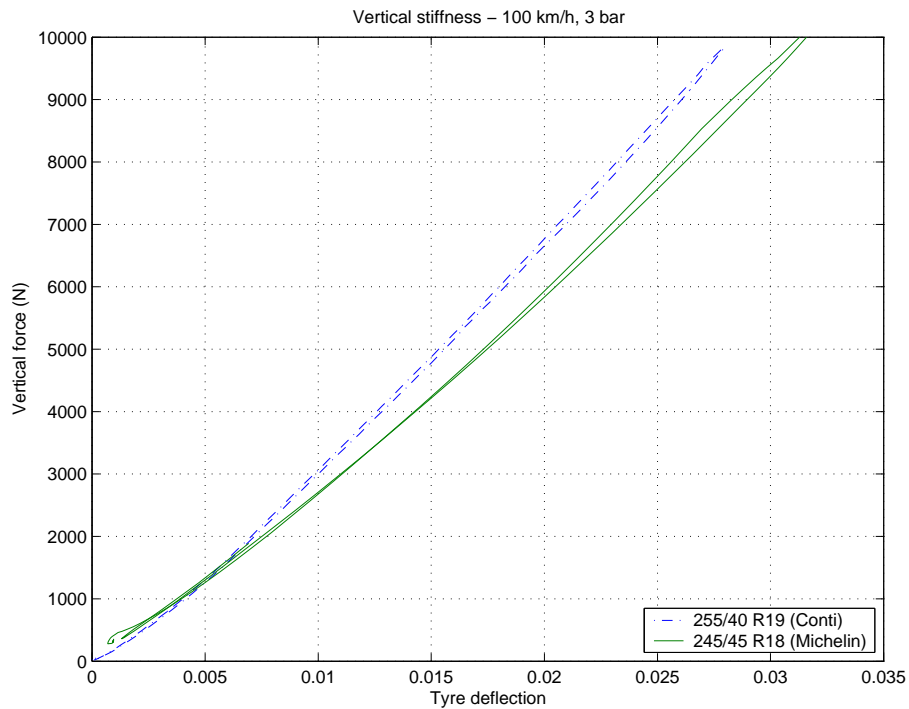


Figure 3.21: Load-deflection relationship for one Michelin Pilot Sport tyre with the dimensions 245/45 R18 and one Conti Sport Contact 2 with the dimensions 255/50 R19 - 100 km/h.

## 3.4 Summary

In this chapter, the influence on the PRW due to both tyre pressure loss and warp has been analysed. The goal was to unravel the problems with the PRW when driving with warp.

According to the results from Section 3.2, false warnings should not occur when driving with warp. Even though *diag*, *fr* and *lr* do change with warp, neither positive nor negative warp should result in any of the PRW's four cases for deflation warning, see Table 2.1. However, it is important to notice that *fr* and *lr* values are not strictly positive or negative. Due to noisy wheel speed signals the values fluctuate with as much as ∼0.4 in absolute value which means that even though, for example, *fr* tends to adopt negative values for negative warp there will still be a quite high portion of positive values. There is a similar behaviour for the *lr* variable. What actually causes the false warnings is the fact that the *diag* value is actually more affected by warp than by 50% tyre pressure loss and will thus exceed the threshold value that has been set in the PRW algorithm for the *diag* value.

The question is still if it will be possible to compensate for warp in the PRW. Both the relationship between the dynamic radius and wheel load and between *diag* and wheel load are fairly linear which indicates that quite a simple compensation should be possible. However, careful attention must be paid to the different load-deflection behaviour shown by different tyre makes and dimensions. The results in Section 3.3 show that tyre deflection is dependent on tyre make, dimension and initial pressure level which are issues that must be taken into consideration when designing a warp compensation.

# Chapter 4

# Warp compensation in PRW algorithm

This chapter brings up how the PRW algorithm can be modified to compensate for warp. A simplified model of the PRW is presented in Section 4.1 and examples of the model outputs are given in Section 4.2. The suggested compensation for warp is described in Section 4.3 and evaluated with the Conti 255/40 R19 tyres in Section 4.4 and with one measurement for the Michelin 245/45 R18 tyres in Section 4.5. The chapter is summarized in Section 4.6.

## 4.1   Simple model of the PRW

Since the PRW software was not available in code and since it was not possible to read any signals from the PRW, a simple model of the PRW is implemented in Simulink based on the information given in the software description [3]. This enables the observation of the PRW variables under the influence of warp or a deflated tyre and the possibility to implement and test a compensation algorithm. The simplified model contains:

- The fundamental logic of the PRW, according to Equations 2.1, 2.2 and 2.3.

- A warning decision strategy according to Table 2.1.

- Speed-dependent offset compensation.

All cases for rejection and cornering compensation are thus ignored. However, the driving manoeuvres will be smooth and calm in all measurement capturing performed for this project, not triggering any of the rejections listed in Section 2.4. Thus, it is a fair assumption that the simplified PRW will, in these tests, behave similar to the real PRW software.

### 4.1.1   Offsets

Even when driving straight ahead with the same velocity, and with the correct pressure in all four tyres, the PRW variables *diag*, *fr* and *lr* will not be centered around zero. This is because there are initial differences in the angular wheel speeds dependent on where the tyres are placed, front or rear axle, due to differences in the sizes of the tyres and small pressure level differences. For this reason, the PRW algorithm contains an offset compensation and this must also be present in the PRW model.

The offset values used in the PRW models have been found by evaluating measurement data from driving straight ahead at three different velocities: 60 km/h, 80 km/h and 120 km/h.

### 4.1.2 Threshold value

As mentioned in Section 2.1, the PRW algorithm contains a threshold value which the variable *diag* must exceed to trigger a tyre pressure deflation warning. The threshold value is, however, not known for the particular test vehicle used in the capturing of measurements for this thesis. Therefore, a suitable value which will be used in the simplified model of the PRW, is derived from test data. The angular wheel speed data captured from driving with one tyre deflated at the pressure level 2.1 bar, which represents 25% deflation, and at 1.5 bar, approximately 50% deflation, is run in the model. Knowing that the PRW can detect a pressure loss of about 30% on one tyre, the threshold value can be adjusted such that the outcome of the model matches this property of the PRW.

The threshold value 0.25 will be used for all the PRW model simulations in this project.

## 4.2 Model output

To see that the simplified PRW model model works correctly, or rather that it gives a reasonable output, it is run for the cases: driving normally, driving with one tyre deflated and driving with warp. The model output test is really to verify that the unknown threshold value has been given a probable value. These results are also good for comparison with the compensation attempt outputs. The model will output four signals, representing the warning variables *FL*, *FR*, *RL* and *RR* (see Table 2.1). The signals will be one if a warning is triggered and zero otherwise.

### 4.2.1 Normal driving

Driving normally, straight ahead, should not trigger any warnings with the simplified PRW model, irrespective of velocity. Measurement data from driving at a velocity of 80 km/h is simulated with the model, the result can be seen in Figure 4.1. The output is zero for all variables throughout the simulation, as it should, with one exception, the variable *RR* goes high for one sample. This is however not enough to trigger a warning since the PRW algorithm builds its warning decision upon a time-based moving average of the latest $k$ algorithm outputs.

### 4.2.2 One tyre deflated

The PRW system should warn correctly when one tyre is 30% deflated, but could also successfully detect a slightly less deflated tyre. In Figure 4.2, the model output from a simulation with a measurement where one tyre, the front right, is 25% deflated can be seen. It is not known exactly how the averaging part of the PRW algorithm is performed, thus it is difficult to determinate whether this output would generate a warning or not. However, it is assumed that the output is close to what the real PRW would output, based on the knowledge that a tyre that is 25% deflated would lie on the border of being detected.

A tyre that is almost 50% deflated should, however, certainly be detected by the PRW algorithm. The model output for a measurement where the front right tyre is almost 50% deflated, can be seen in Figure 4.3 and it is here quite clear that this output would generate a warning.
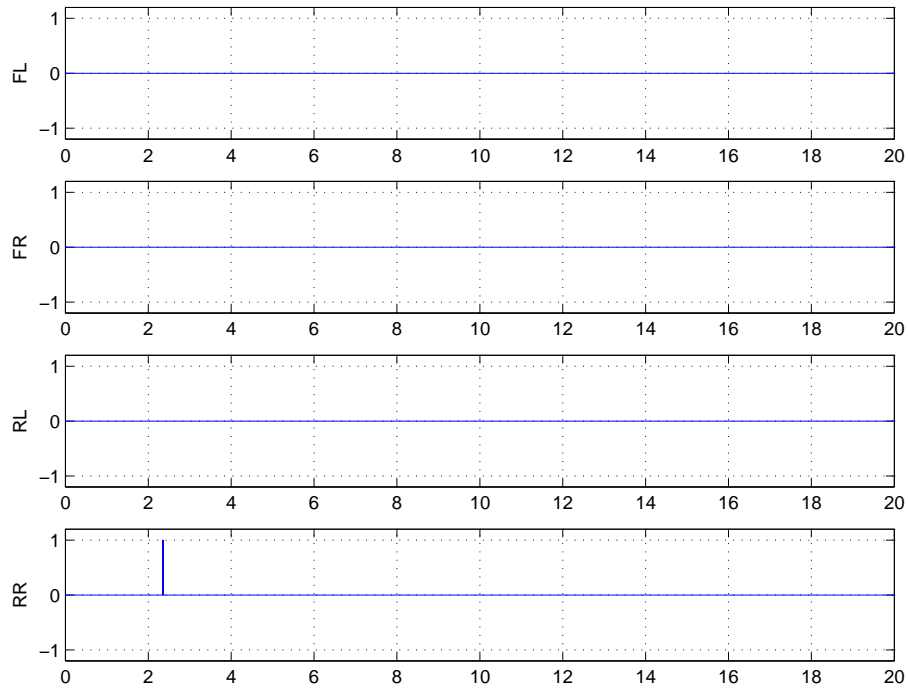
Figure 4.1: PRW model simulation output over time (s), normal driving at 80 km/h.
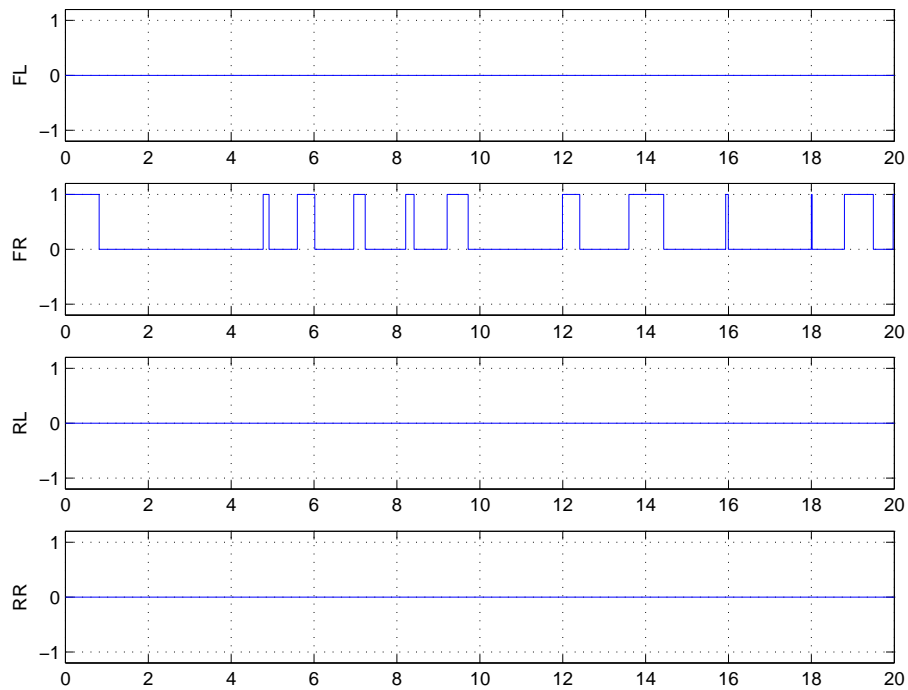


Figure 4.2: PRW model simulation output over time (s), normal driving at 80 km/h with the front right tyre pressure level at 2.1 bar (25% deflation, all other tyres 2.8 bar).
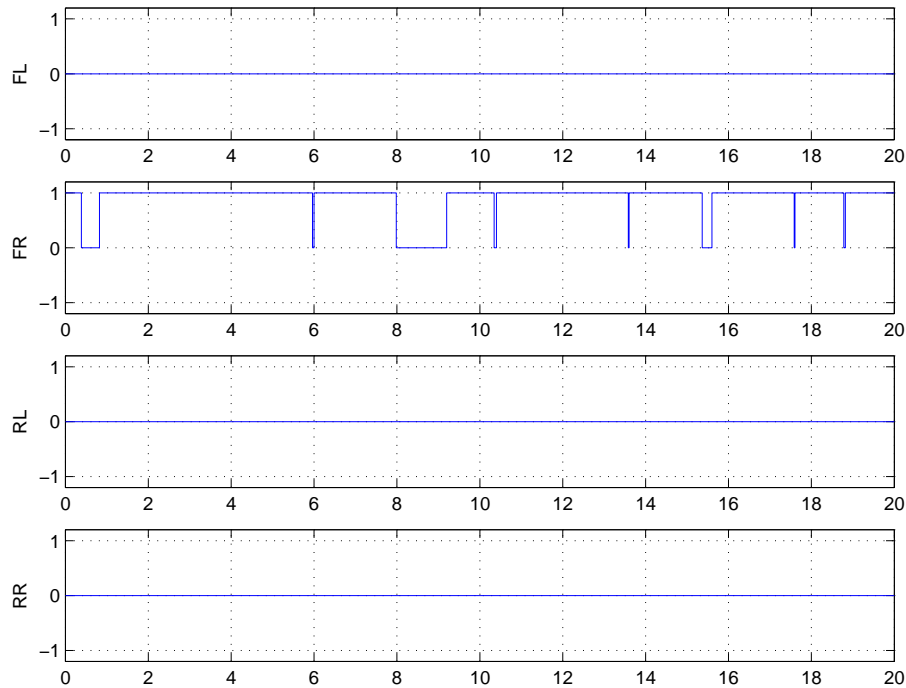
Figure 4.3: PRW model simulation output over time (s), normal driving at 80 km/h with the front right tyre pressure level at 1.5 bar (about 50% deflation, all other tyres 2.8 bar).

### 4.2.3 Driving with warp

The PRW model output, simulated with a measurement captured when driving with constant warp, can be seen in Figure 4.4. See Figure 4.5 for an example of a constant negative warp force. Also here, it is difficult to say if this is enough to trigger a warning, but it is clear that warp has influenced the output. The reason that only $FR$ and $RL$ variables are affected is that for this measurement, negative constant warp has been applied and according to the theoretical argument presented in Section 3.1.1, the PRW variable $diag$ will decrease with negative warp. Looking then at the rules from which the PRW algorithm makes its decision, see Table 2.1, a negative $diag$ value could generate either a $FR$ or a $RL$ warning.

### 4.2.4 One tyre deflated with warp

Figure 4.6 shows what could happen when warp is applied when driving with one deflated tyre. For this measurement, the right tyre had a pressure of 1.5 bar, corresponding to about 50% less pressure than the other tyres. Warp was constant, negative for the first half of the measurement and positive for the second half, see Figure 4.7. The PRW model is supposed to clearly warn for a pressure loss at the front right tyre, but this is not the case for the part of the measurement with a constant positive warp. Positive warp increases wheel load on the front left and rear right wheels, meaning that angular wheel speeds increase, and decreases wheel load on the front right and rear left wheels, where angular wheel speeds will decrease. The positive constant warp will thus compensate for the increase in wheel speed caused by the front right deflated tyre, and the PRW algorithm will, under these circumstances, not recognize the loss in pressure.

37
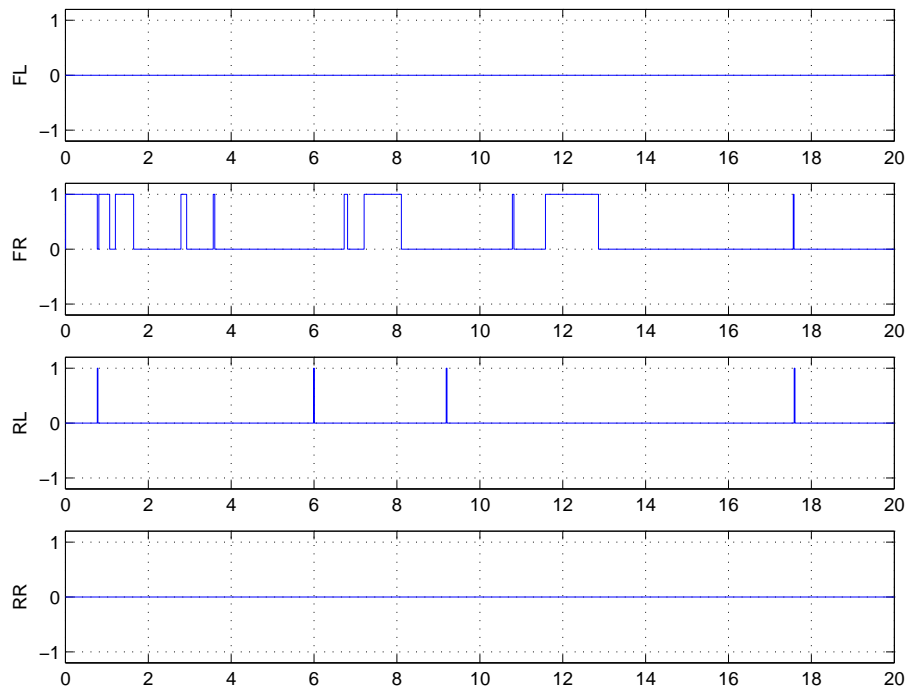
Figure 4.4: PRW model simulation output over time (s), driving with constant negative warp of 10 kN at 80 km/h.
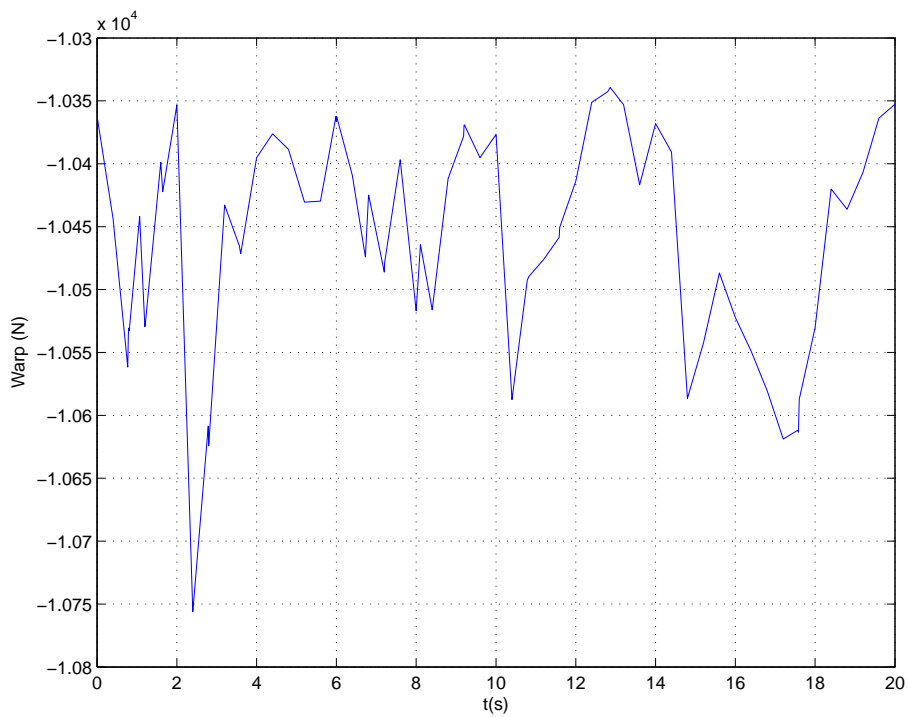


Figure 4.5: Constant negative warp of 10 kN over time (s).
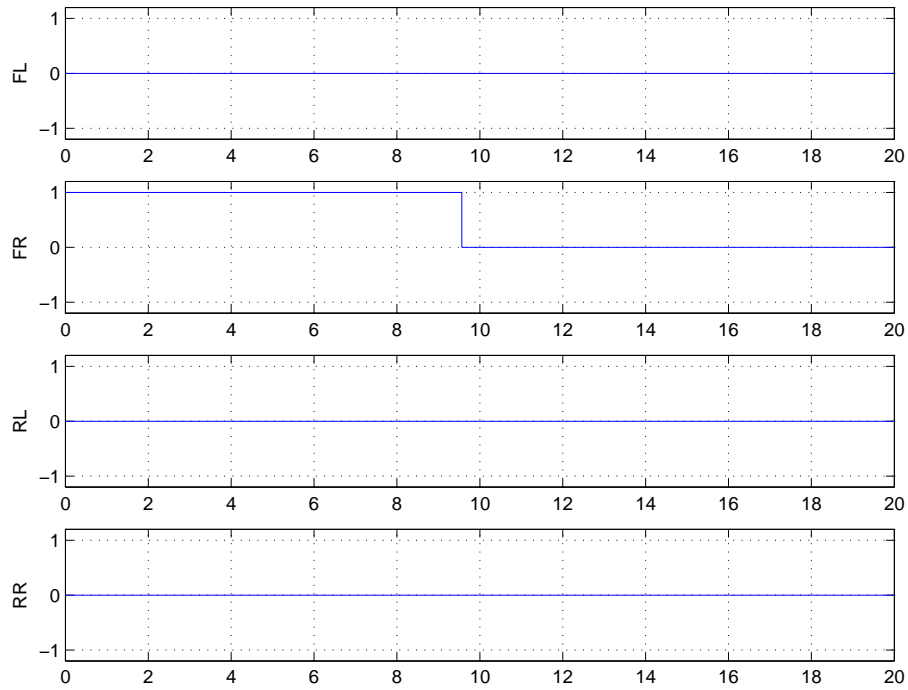
Figure 4.6: PRW model simulation output over time (s), driving with constant positive and negative warp of 12 kN at 80 km/h, the front right tyre with almost 50% pressure loss.
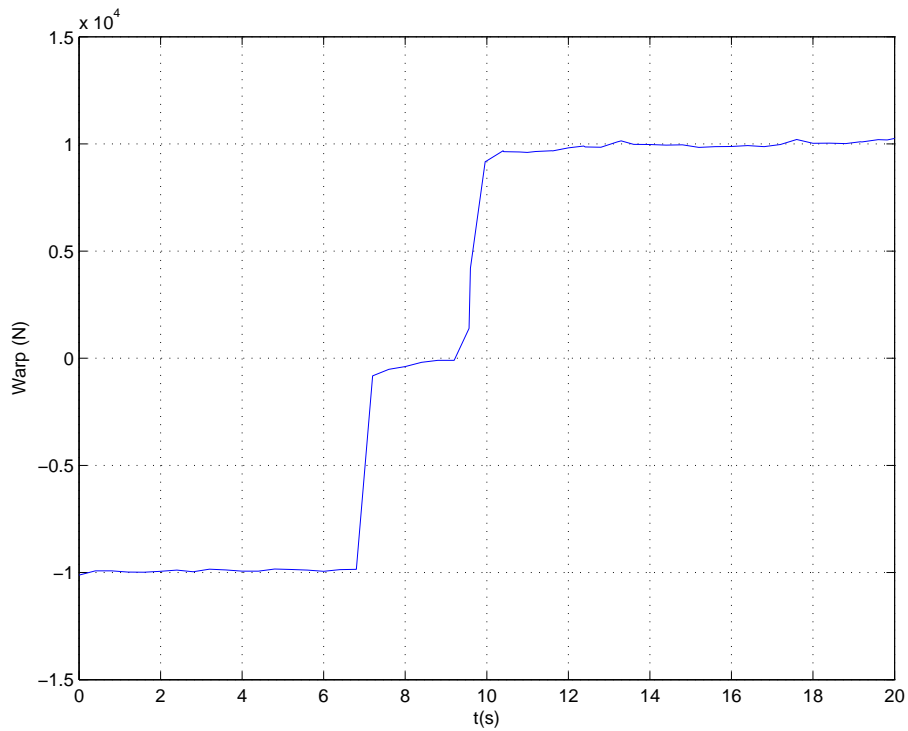


Figure 4.7: Constant warp, negative and positive, of 12 kN over time (s).

## 4.3 Correction in PRW algorithm

The results from the previous chapter indicate that a compensation for warp should be possible under the assumption that the initial tyre pressure level, the tyre dimensions and the make is known. One method for warp compensation will be analysed in this section. The compensation strategy is based on the test results from Section 3.2 and therefore only apply to the particular tyres and test vehicle used to derive these results. The general idea for the compensation method, however, should be applicable for any tyre under the assumptions mentioned above.

### 4.3.1 Choice of compensation strategy

The PRW uses the angular wheel speeds to calculate the PRW variables *diag*, *fr* and *lr* which determine if a tyre is deflated through the warning strategy presented in Table 2.1. It is therefore desirable to find a compensation strategy which alters either the wheel speed signals before being used in the PRW algorithm or the PRW variables themselves.

It is known that warp changes the dynamic radius and also by how much. The altered wheel speed due to warp for wheel $i$, $\omega_{i,new}$, can be calculated with the average velocity and the altered dynamic radius, $r_{i,new}$, as:

$$\omega_{i,new} = \frac{v_x}{r_{i,new}}$$

where

$$\omega_{i,new} = \omega_{i,old} + \Delta\omega_i$$

and

$$r_{i,new} = r_{i,old} + \Delta r_i$$

Consequently, the change in wheel speed can be expressed as:

$$\Delta\omega_i = \frac{v_{x,i}}{r_{i,old} + \Delta r_i} - \omega_{i,old}$$

To calculate the change in wheel speed for each wheel the dynamic radius and the wheel speed without warp and at the correct pressure level and velocity must be known. This makes compensation for warp directly on wheel speeds impractical, if not impossible. Instead, the relationship between the PRW variable *diag* and wheel load can be used. This has the advantage that the compensation only has to provide one value and that this value can be derived using only the warp signal. This compensation idea will be presented in the following section.

### 4.3.2 The warp compensation method

The relationship between warp and the PRW variable *diag* is known from the previous chapter. There it was established that there is an approximately linear dependency between them and using this fact makes a compensation fairly straightforward. Since the relationship is velocity dependent, a linear approximation is made for three different velocities: 60 km/h, 80 km/h and 120 km/h. An example of a linear approximation of *diag* as a function of warp can be seen in Figure 4.8. One remark to the figure is that offset has not been deducted from the *diag* value before the linear approximation. When the linear approximation is to be used in the
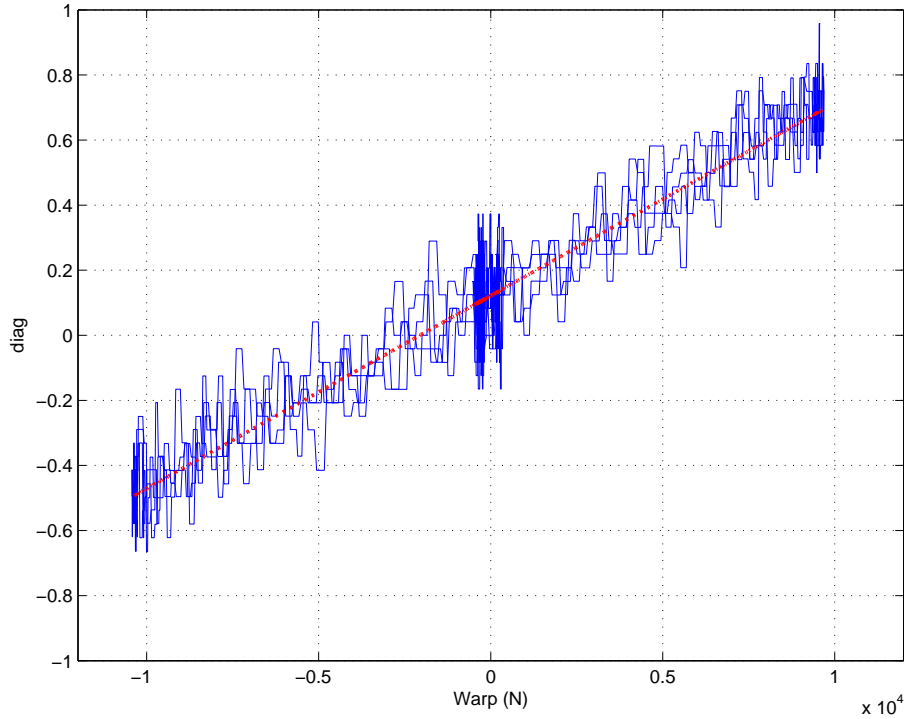
Figure 4.8: *diag* variable as a function of warp with a polynomial fit of degree one.

compensation algorithm, the y-intercept will be set to zero since, for zero warp, compensation should also be zero. This offset is already deducted in the original PRW algorithm. With the wheel load signals, the change in *diag* due to warp can be derived which then can be deducted from the calculated *diag* value, before this is used in the PRW warning decision logic.

## 4.4 Evaluation of new algorithm

The warp compensation strategy will be evaluated by simulation with measurement data. The algorithm is thus run offline with the appropriate data captured with a vehicle on a test track. The same data, which was evaluated with the PRW model without warp compensation in the previous section, will be used also for the corresponding cases in this section. This facilitates the comparison between the two models.

### 4.4.1 Normal driving

The warp compensation must not interfere when driving normally, without the warp application running. Looking at the relationship between *diag* and warp, on which the algorithm is built, for zero warp the compensation should also be zero. This is verified by the simulated output which can be seen in Figure 4.9.

### 4.4.2 Low pressure on one tyre

The main functionality of the PRW may not be disturbed by the warp compensation algorithm. Thus, the detection of a low pressure on one tyre should not be affected by the compensation
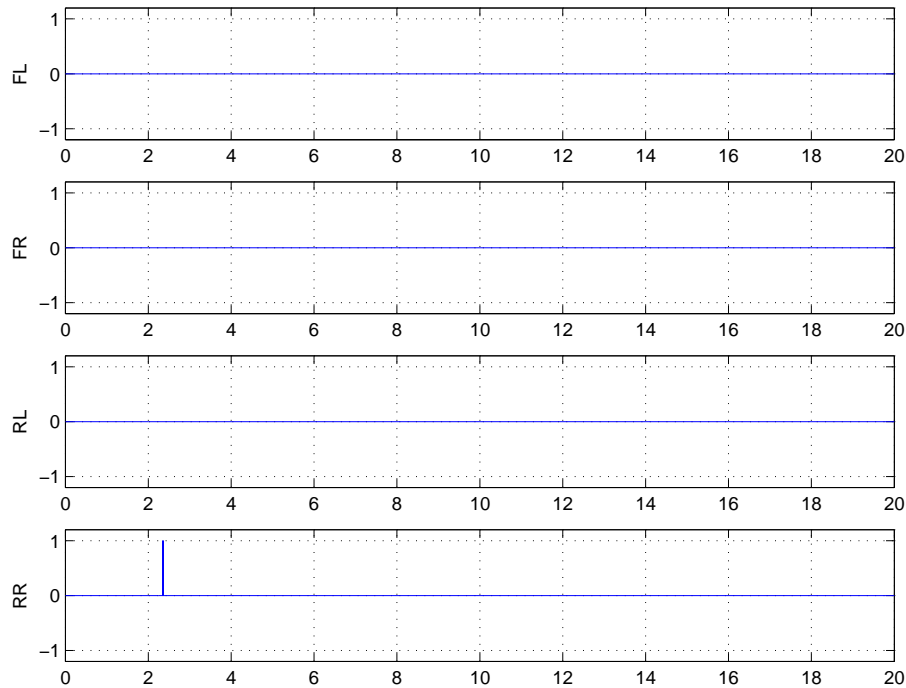
Figure 4.9: Simulation output over time (s) for the PRW model with warp compensation, driving normally at 80 km/h.

algorithm when the warp application is not active. Preferably, the outcome of the PRW model with compensation, for this case, should be the same as the for the PRW model without compensation. This is also the case, as can be seen in Figure 4.10 for one tyre, front right, 25% deflated and in Figure 4.11 for the same tyre almost 50% deflated.

### 4.4.3 Driving with warp

When driving with warp, the algorithm should ideally suppress all influence on the PRW warning variables caused by warp. To test the compensation, maximum wheel load level for driving with constant negative warp, see Figure 4.5, is investigated. The result can be seen in Figure 4.12 and shows that almost all warnings triggered by warp, as was demonstrated in the previous section in Figure 4.4, are suppressed.

### 4.4.4 Low pressure on one tyre and driving with warp

It should be possible for the PRW to detect a low pressure on one tyre when driving with warp. Hence, it is necessary to make sure that the compensation does not influence the PRW such that a low pressure warning is overlooked. At the same time, it is desirable that the compensation also corrects the problem shown in the previous section, a constant warp hiding a loss in pressure from the PRW through decreasing wheel load on that particular wheel. Figure 4.13, shows the model output from driving with warp and having a 50% pressure loss on the front right tyre. Here, the deflation warning is on for the front right tyre which indicates that the compensation both works with a loss in pressure on one tyre and can recompensate for warp such that the warning no longer is hidden.
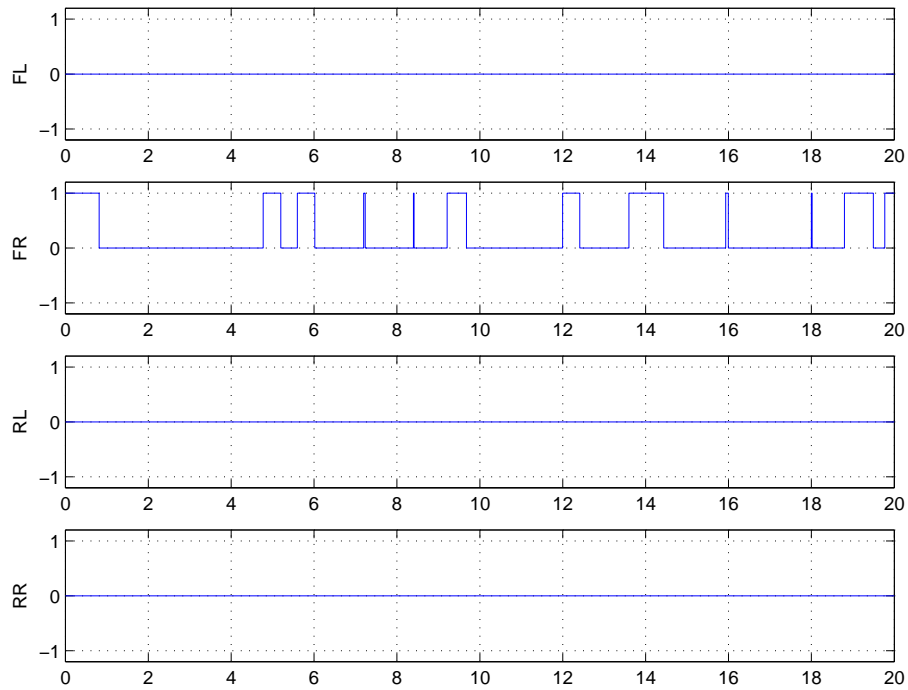
Figure 4.10: Simulation output over time (s) for the PRW model with warp compensation with the front right tyre pressure 25% deflated at 2.1 bar with all other tyres at 2.8 bar. Velocity is 80 km/h.
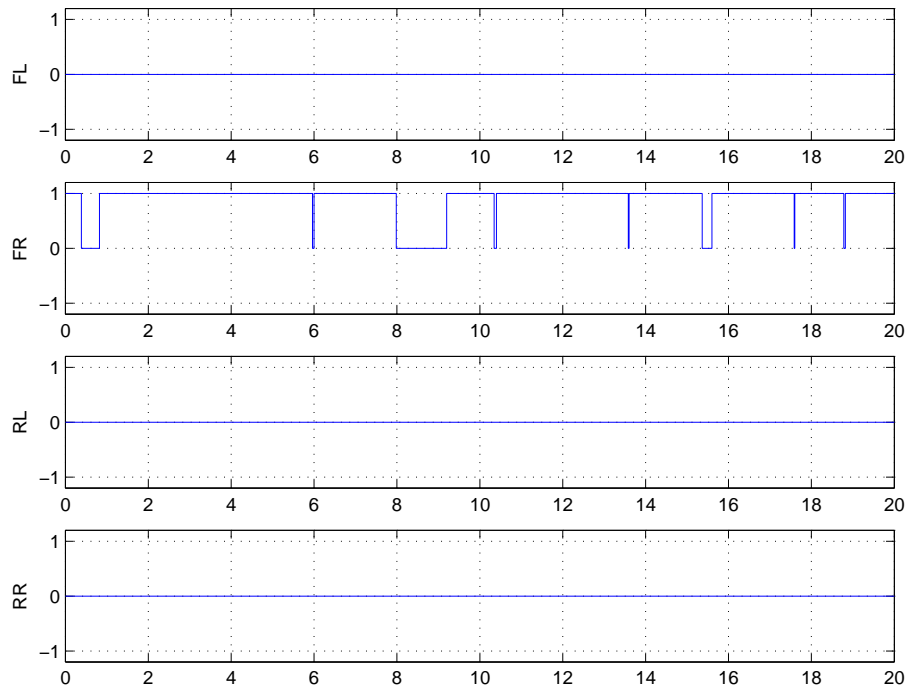


Figure 4.11: Simulation output over time (s) for the PRW model with warp compensation with the front right tyre pressure about 50% deflated at 1.5 bar with all other tyres at 2.8 bar. Velocity is 80 km/h.
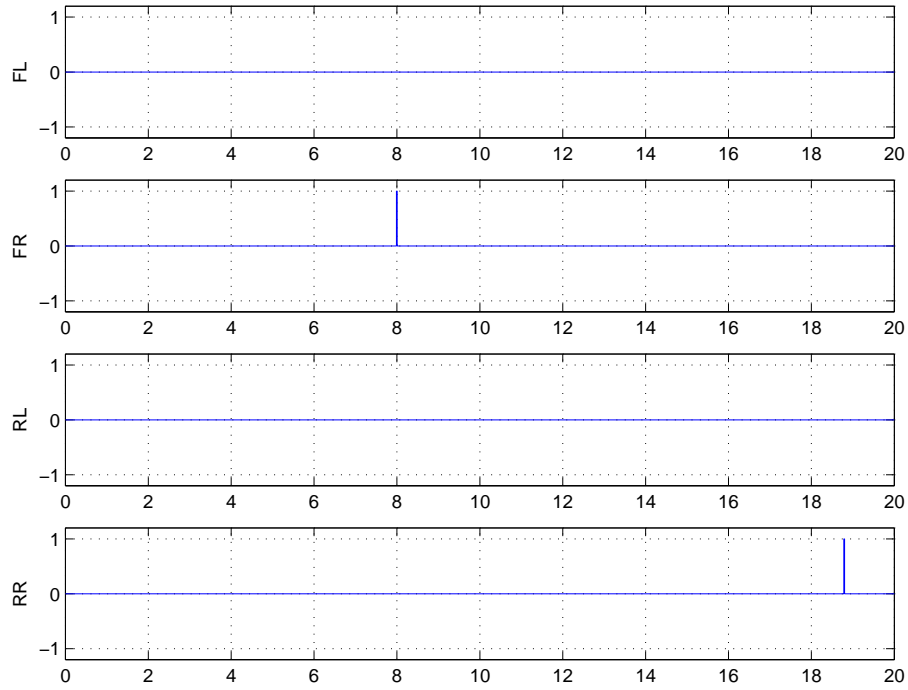
Figure 4.12: Simulation output over time (s) for the PRW model with warp compensation, driving with constant negative warp at 80 km/h.
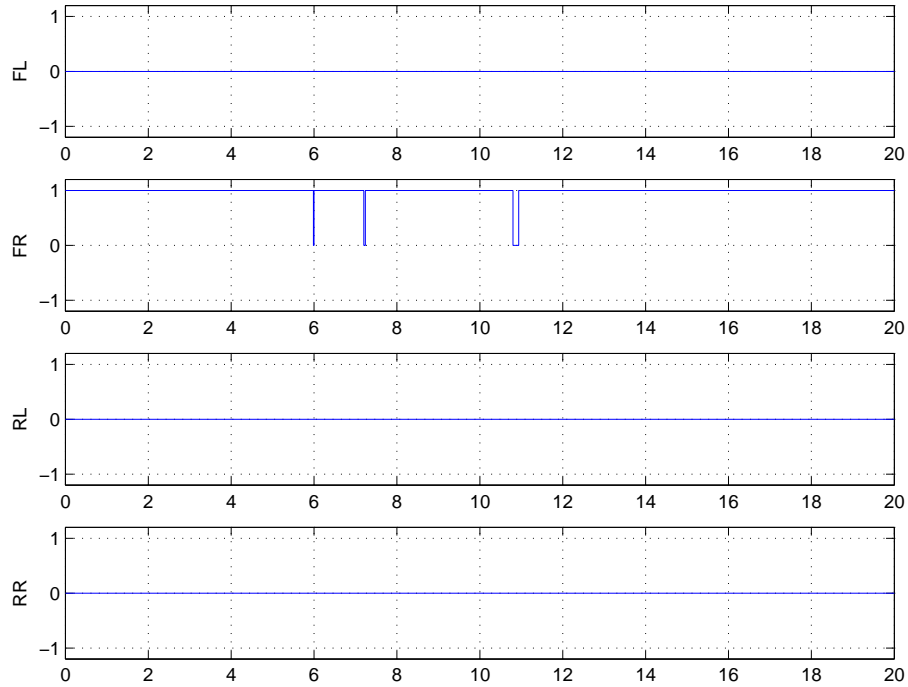


Figure 4.13: Simulation output over time (s) for the PRW model with warp compensation with the front right tyre pressure about 50% deflated at 1.5 bar with all other tyres at 2.8 bar, driving with constant warp at 80 km/h.

## 4.5 Compensation tolerance with different types of tyres

In the previous chapter, Section 3.3, the tyre deflection as a function of wheel load was investigated for several different tyres. There it was established that there could exist quite a large difference between different tyres, depending on tyre make, dimension and initial pressure levels. Preferably, a warp compensation algorithm should work for all tyres such that only one implementation is sufficient for any possible type of tyre that the vehicle may have. Therefore, as the compensation suggested here has been derived from measurements with one specific set of tyres, to investigate the robustness of the algorithm it should be tried out on other tyres as well.

### 4.5.1 Comparison between the Conti 255/50 R19 and Michelin 245/45 R18 tyre

To test the tolerance for the warp compensation algorithm presented in this report, one measurement with Michelin 245/45 R18 tyres will be simulated with the PRW model. This measurement is captured when driving on a test track with warp at a velocity of 80 km/h. The tyre pressure was normal on all tyres. The warp signal can be seen in Figure 4.14.
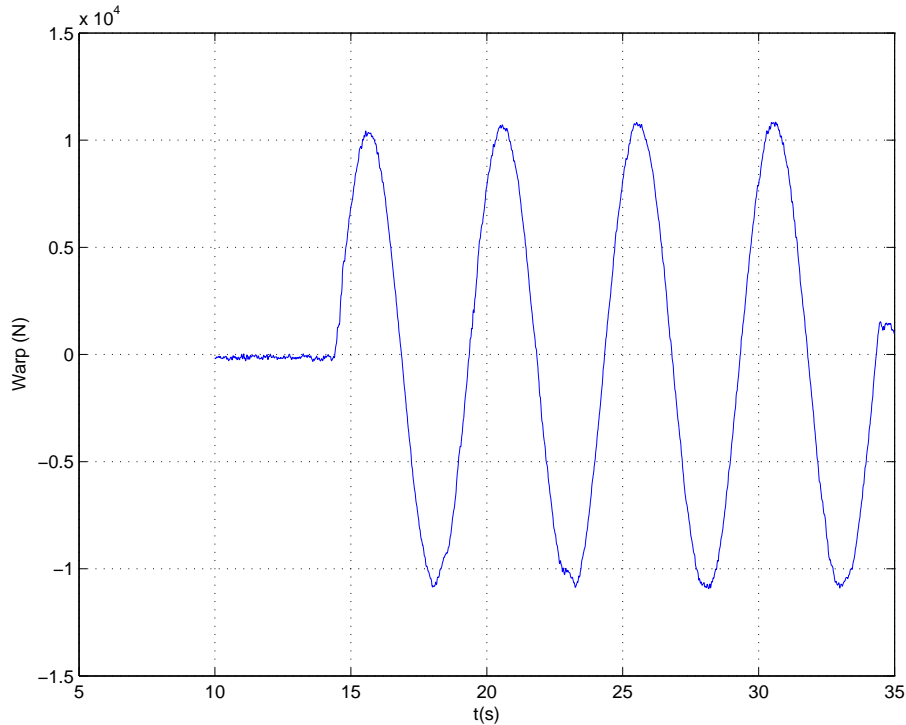


Figure 4.14: Warp force applied in the measurement for the Michelin tyre.

In Section 3.3.5, this Michelin tyre and the tyre for which the warp compensation algorithm is built, are compared. For example, Figure 3.20 reveals that the difference in tyre deflection as a function of wheel load between the two tyres is quite large. Also, looking at the dynamic radius as a function of wheel load, the different behaviour between the two is quite obvious. Figure 4.15 shows the dynamic radius as a function of wheel load for the Michelin tyre which

appears fairly different compared to the Conti tyre, see Section 3.2.3.
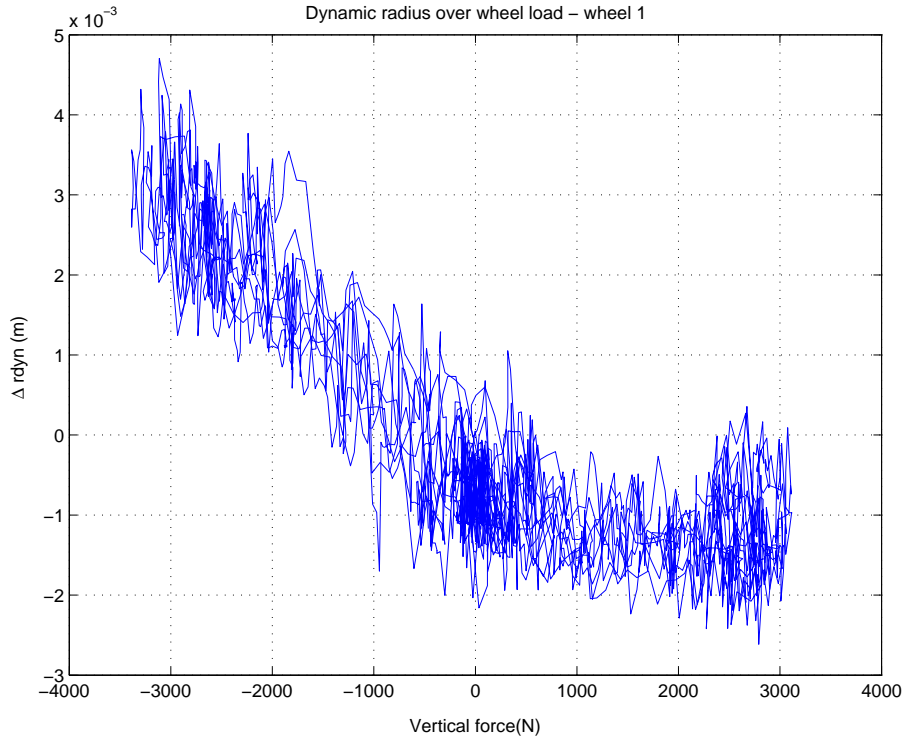


Figure 4.15: Dynamic radius as a function of wheel load for wheel 1 (front left) for the measurement with the Michelin tyre.

The relationship between the PRW variable *diag* and warp, which is used in the warp compensation algorithm, can be seen for the Michelin tyre in Figure 4.16. This seems to hold a similar linear relationship as for the Conti tyre, but with a steeper gradient and a different offset. In exact numbers, the linear approximation for *diag* as a function of warp with the Michelin tyre has a gradient of $6.575 \cdot 10^{-5}$ which can be compared with $5.964 \cdot 10^{-5}$ which was evaluated for the Conti tyre in Section 3.2.5.

### 4.5.2 The warp compensation algorithm with the Michelin tyre

The warp compensation, i.e. the functional relationship *diag* over warp, may not be changed to fit the Michelin tyre. The offset values, however, must be altered since they are not a part of the compensation algorithm and without correct offsets the PRW model will not work properly. The offsets are derived by the PRW algorithm as soon as the tyres are changed and they are thus always adjusted to the current tyre set.

The measurement simulated with the PRW model without warp compensation can be seen in Figure 4.17. The warning indications are quite frequent during warp, but absent for the first 15 seconds which is a good sign since this means that the PRW model works correctly also when there is no warp. With this, it can be assumed that the offset and threshold values are about right.
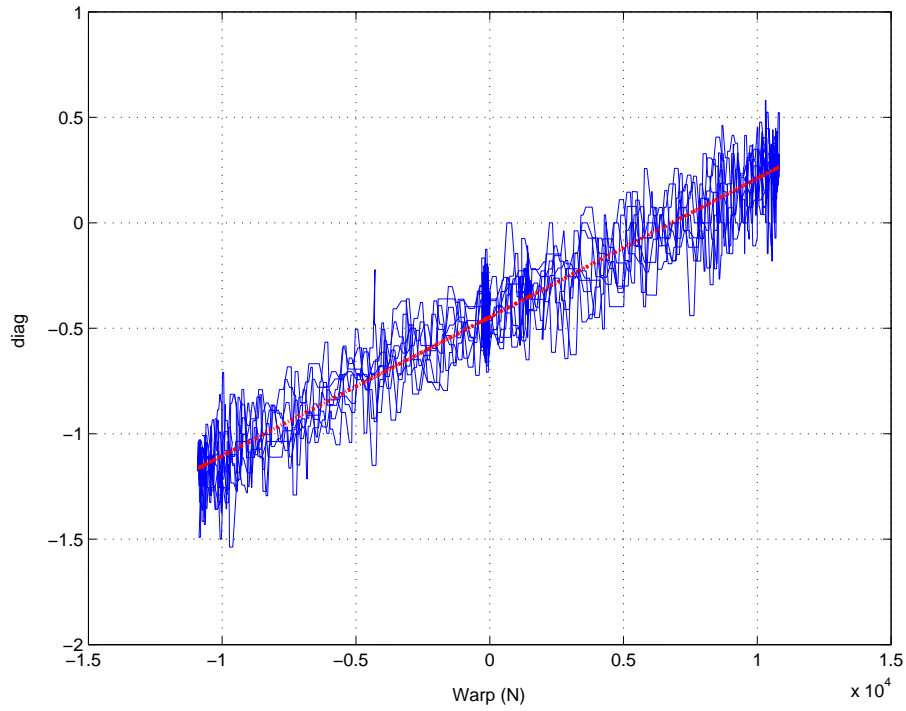
Figure 4.16: The PRW variable *diag* as a function of warp for the measurement with the Michelin tyre.
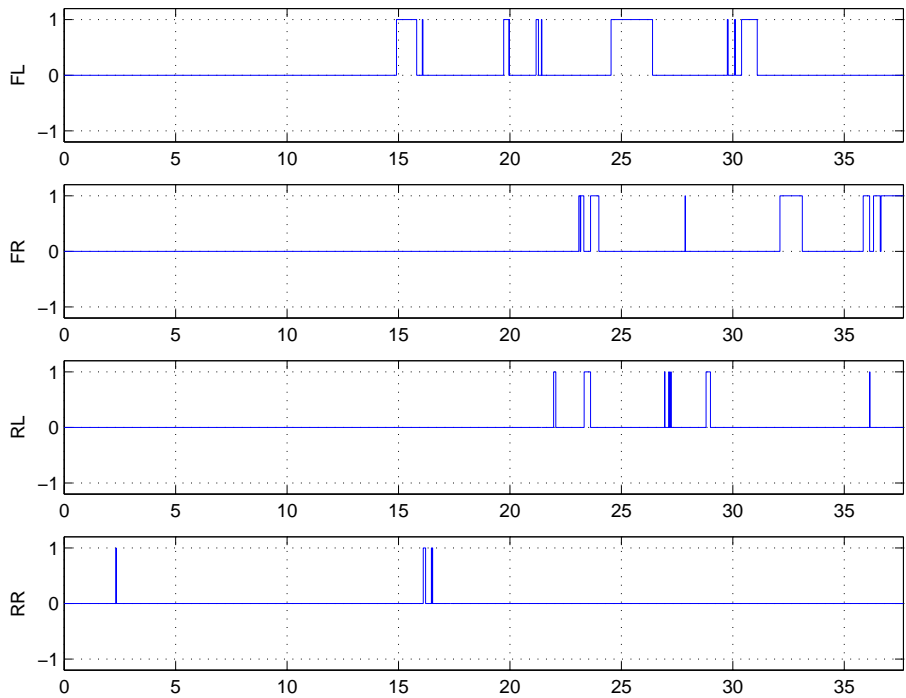


Figure 4.17: Output from the PRW model over time (s), without warp compensation, for the measurement with the Michelin tyre. The warp signal was sinusoid, see Figure 4.14.

In Figure 4.18 the measurement with Michelin tyres simulated with the PRW model with warp compensation can be seen. The compensation seems to work surprisingly well for these tyres, considering the difference of the tyre deflection curves. The number of warning indications left after the compensation are not so different compared to the results with the Conti tyres.
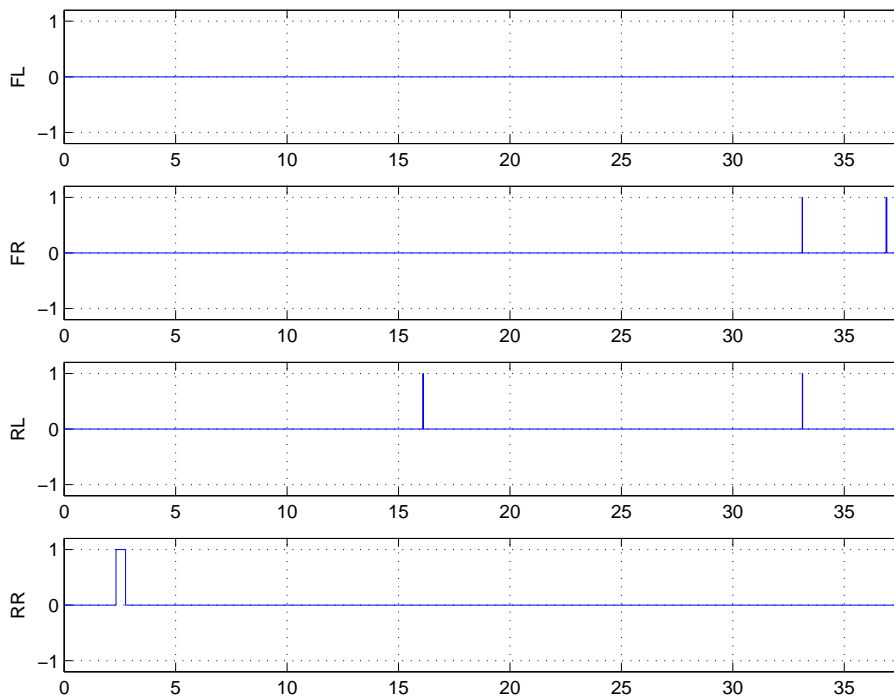


Figure 4.18: Output from the PRW model over time (s), with warp compensation, for the measurement with the Michelin tyre. The warp signal was sinusoid, see Figure 4.14.

## 4.6 Summary

In this chapter, the PRW model and the warp compensation algorithm for the PRW were presented and evaluated with offline simulations. The compensation was developed to suit the S-class with Conti 255/40 R19 tyres, which is the vehicle and tyres used for testing and measurement capturing throughout this thesis. Finally, the compensation was also tried for a measurement with another set of tyres than the compensation was developed for.

In general, for the Conti tyres, the warp compensation seemed to be able to suppress the influences from warp on the PRW functionality. Target for investigation has been a constant warp force since this is the worst case for the PRW. The compensation also worked fine when using measurements captured with the Michelin 245/45 R18 tyres, which is a promising result.

Although it is certain that the results achieved in this chapter do reflect the problems and possible solutions concerning the PRW and warp, there are some details concerning the implementation of the PRW model that must be taken into consideration. These are the values of the offsets, the threshold and the warning decision functionality. All three are more or less estimated and therefore it is difficult to comment on the accuracy of the model. It is probable that the offset values are very important for a correct behaviour, but it is hard to

tell whether the offsets generated and used here are more or less accurate than they would be in the real PRW. The value of the threshold is also estimated and most likely the value is set a bit too high, but it could also have been set too low. Finally, the warning strategy used here is a simplified version of how it is implemented in the real algorithm and how much this affects the result is also difficult to say.

# Chapter 5

# Applications

In this chapter, the PRW model and particularly the warp compensation algorithm, will be analysed offline with two applications for warp. First, in Section 5.1, a description of warp and the active suspension system is made. In Section 5.2 the application topic *Road bank assistance* is presented and tested, followed by *Lane-keeping* in Section 5.3. The chapter ends with a summary in Section 5.4.

## 5.1 Warp theory

### 5.1.1 The ABC system

Present in some Mercedes cars is the ABC system which is an active suspension system with the purpose to enhance comfort for the driver and the passengers, without worsening handling properties. Another feature is that the system can be adapted such that different driver preferences concerning the suspension can be met. The ABC system aims to reduce the vehicle's vertical and horizontal oscillation movement of the body in order to achieve improved ride comfort. This is implemented by applying a certain amount of extra vertical force at each wheel which is controlled by the system. The vertical forces on each wheel are produced by a high-pressure hydraulic system where oil is fed from a pump to a hydraulic cylinder. The wheel loads can thus be changed by controlling the amount of oil from the pump to each wheel's cylinder [5].

### 5.1.2 Warp

As mentioned in the introduction, warp is the manipulation of a vehicle's steering properties achieved by controlling the vertical forces at each wheel through the ABC system. Again, total warp is the sum of the additional wheel loads:

$$warp = F_{z,1} - F_{z,2} - F_{z,3} + F_{z,4}$$

where $F_{z,i}, i = 1...4$ are the additional wheel loads for each wheel respectively.

The sum of vertical force at all wheels is constant, which means that the maximum amount of additional wheel load at one wheel is restricted to how much that can be deducted at another wheel. Also, the manoeuvre must not introduce a rotating force in latitudinal or longitudinal direction, i.e. pitch or roll movement. Consequently, the amount of wheel load added or

deducted at each wheel must be the same for all four wheels, that is, if $F_{z,i}$ is the added or deducted wheel load on wheel $i$ then

$$|F_{z,i}| = \frac{warp}{4}$$

Further, positive wheel load on wheel 1 (front left) can only be combined with positive wheel load on wheel 4 (rear right) and negative wheel load on wheel 2 and 3 (front right and rear left respectively). This is referred to as a positive warp. A negative warp is accordingly negative wheel load on wheel 1 and 4, positive wheel load on wheel 2 and 3.

The amount of warp that can be applied can also be restricted by the suspension system. In this project, maximum warp force is restricted to 12 kN, hence, maximum additional wheel load on one wheel is at most 3000 N.

## 5.2   Road bank assistance

One of the possible applications for warp is to assist the driver in the presence of road bank. This is a slight slant of the road which, without steering correction, will make the vehicle drift towards the base of the slant. Warp can be used to compensate for the road bank without having to interfere with the steering wheel angle.

### 5.2.1   General functionality

The main idea for road bank assistance is to detect road bank and apply a certain warp to compensate. Sensor signals from the ESP system are compared with a model output and the difference between them is recognized as a disturbance due to road bank. The amount of road bank, expressed in degrees, is then used together with the current velocity in another model to calculate the warp needed to correct for the road bank disturbance.

### 5.2.2   Influence on the PRW by road bank assistance

One important conclusion in Chapter 3 was that the PRW functionality is most affected by constant warp under a longer period of time. This is most relevant in the case of road bank assistance since a slight road bank could very well occur for a significant stretch which would mean that a constant warp must be applied for this time.

To examine the effect on the PRW from road bank assistance, measurements from a test drive where road bank is present have been run through the simplified PRW model with the warp compensation which was presented in Chapter 4. The estimated and measured road bank can be seen in Figure 5.3 and calculated warp that was needed to correct for this road bank can be seen in Figure 5.1. As was mentioned earlier, the limit for when the PRW will incorrectly warn for low pressure is between 750 and 1000 N on each wheel, that is, a total warp force of 3000–4000 N. Here, the maximum warp level is at slightly over 3000 N which then should be on the border of causing a false warning. This is reflected in PRW model output, which can be seen in Figure 5.2. It is also worth noticing how the PRW model does not react to the first half of the measurement, where there is a warp level of around 2000 N, however, when in the second half warp increases to over 3000 N the false warnings appear.
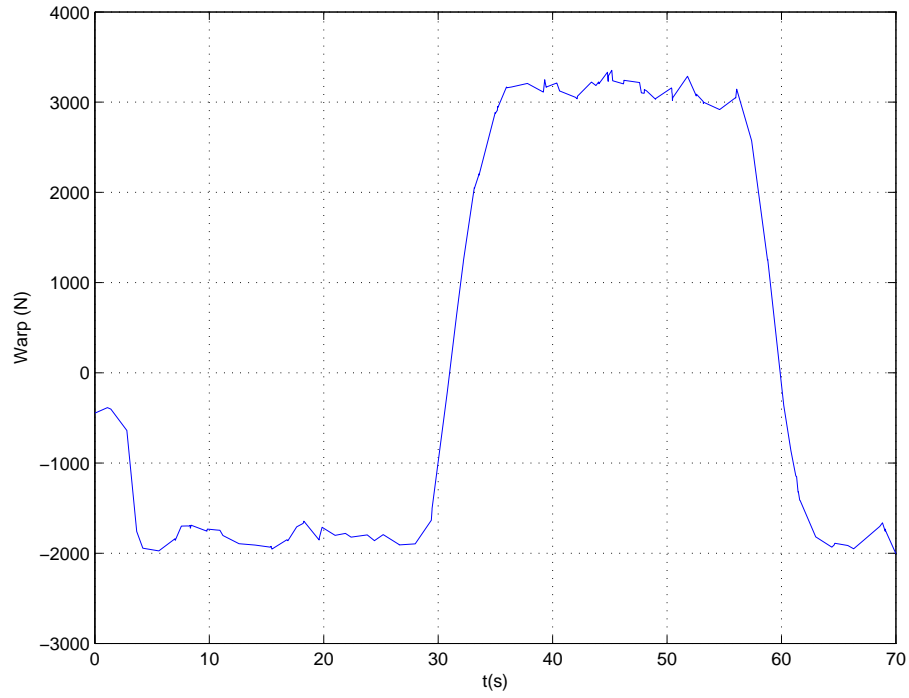
Figure 5.1: Applied warp needed to compensate for road bank.



Figure 5.2: PRW model output, without warp compensation, simulated with measurement data from driving with road bank assistance active.
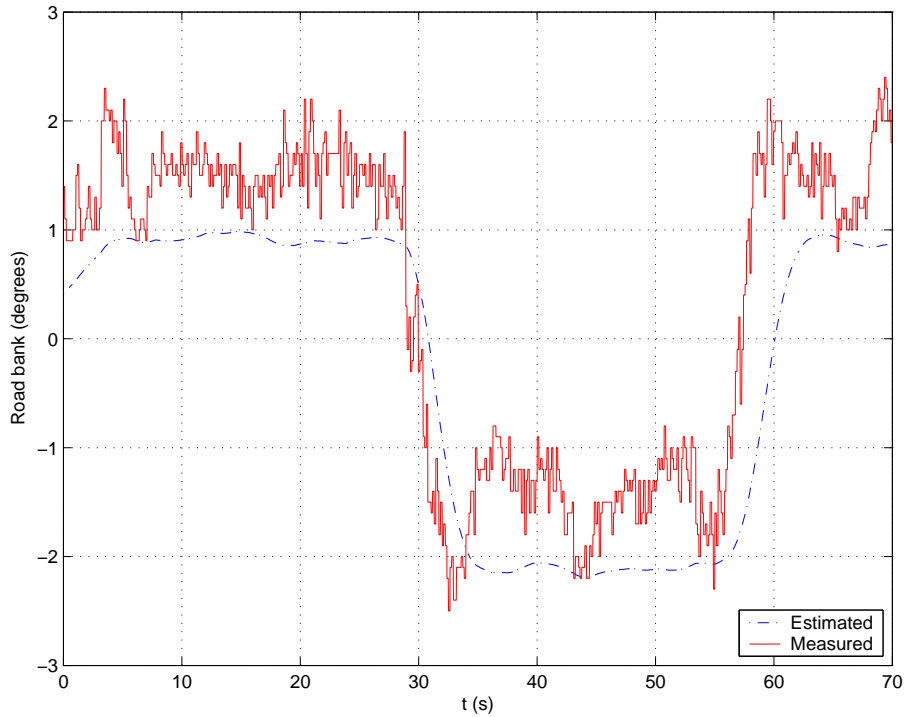
Figure 5.3: Size of road bank, estimated and measured values, in degrees.

### 5.2.3 Road bank assistance with warp compensation

Figure 5.4 shows the PRW model output for the same measurement as was used in the previous section. The warp compensation manages to take care of nearly all cases of the warning signals going high. The occurrence of warning signal for the rear left at the end of the sequence can be explained by looking at the velocity, see Figure 5.5. At the end of the measurement the velocity drops quite fast meaning that the PRW model will not work properly since it is developed for a constant or slowly changing velocity.

## 5.3 Lane-keeping

Another application for warp is lane-keeping, which is intended to support the driver to follow one lane. It is not an autonomous system, meaning that the vehicle will not be kept in lane by the application without any driver interference at all. The system is aimed mainly at assisting the driver such that less effort will be needed to keep the car within the lane.

### 5.3.1 General functionality

The lane-keeping application uses an optical night view camera to establish the vehicle's position within its current track. A track recognition algorithm uses these position coordinates to evaluate parameters which in turn will be used in a controller. The controller outputs the desired yaw rate, which the vehicle should fulfill to stay in the lane. This yaw rate is then used to calculate the appropriate warp force.
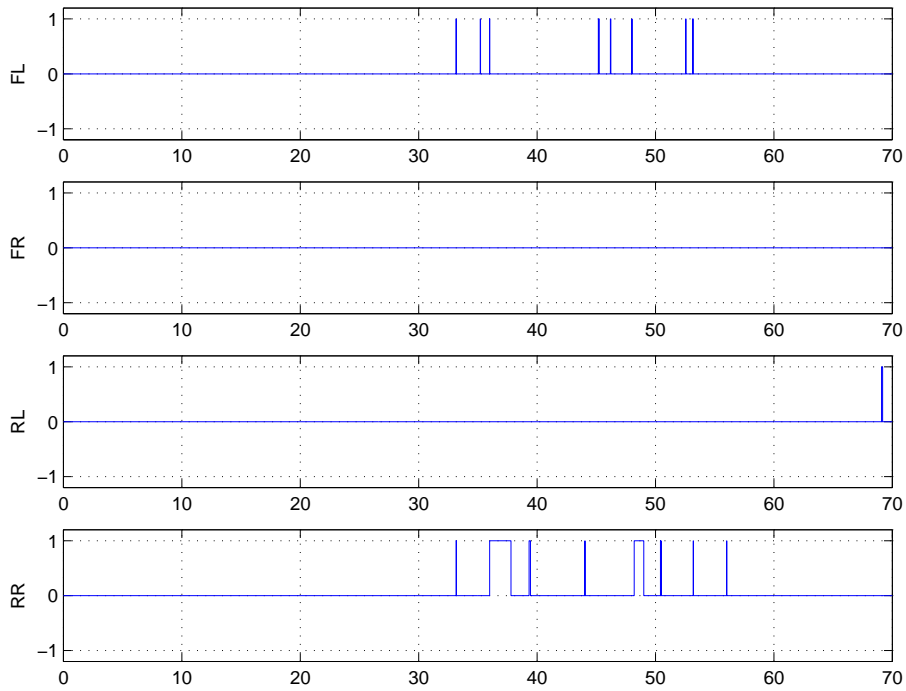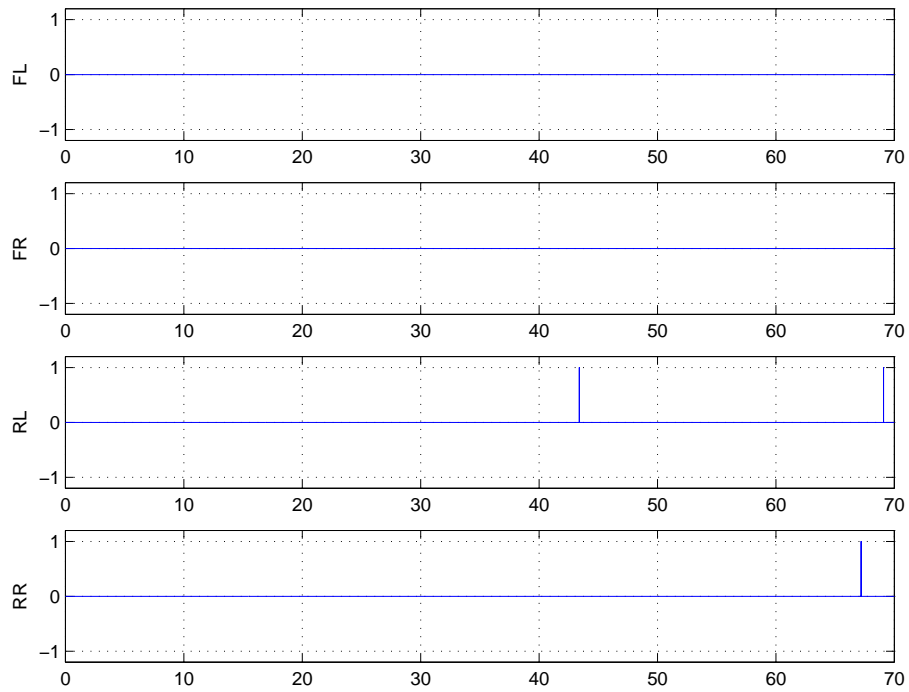
Figure 5.4: PRW model output, with warp compensation, simulated with measurement data from driving with road bank assistance active.
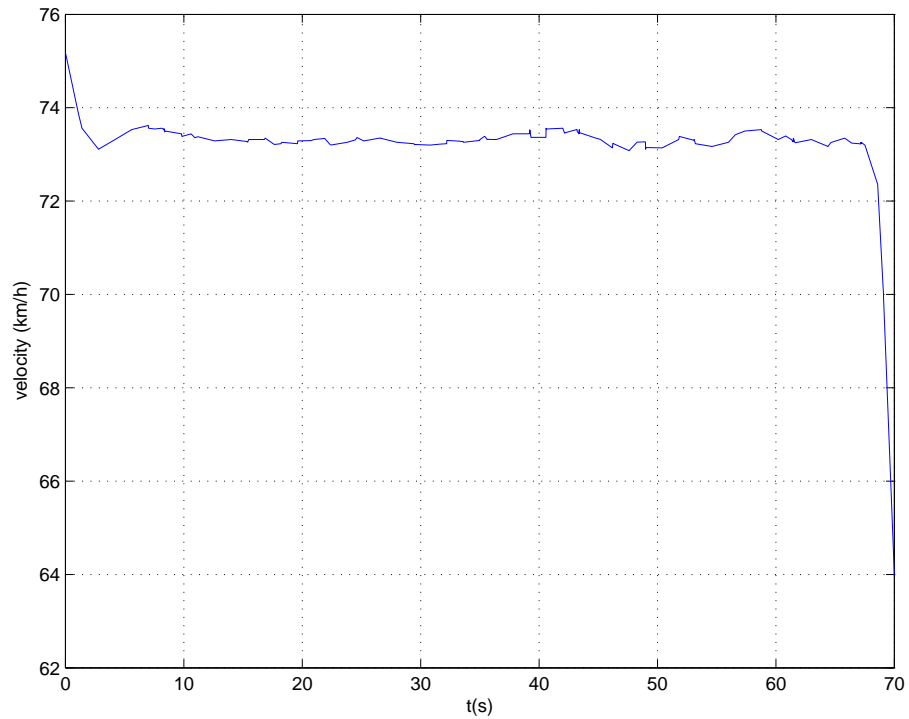


Figure 5.5: Velocity of vehicle, from measurement data captured when driving with road bank assistance.

### 5.3.2 Influence on the PRW by lane-keeping assistance

As with the road bank application, a constant warp during a longer period of time can be necessary also for this application. Consider, for example, a part of a road with a long curve. To follow such a road pattern a constant warp must be applied. It is thus likely that the false warnings from PRW could occur for this application as well.
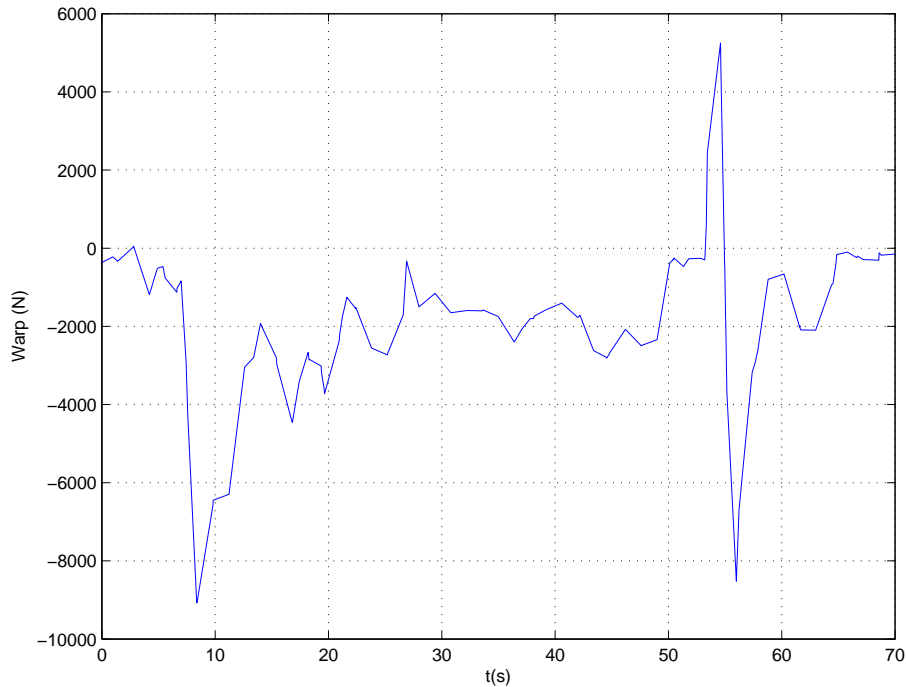


Figure 5.6: Warp force needed for lane-keeping, measurement 1.

Two different measurements have been analysed for the lane-keeping application. In the first measurement, the lane to follow is fairly straight and the applied warp force is therefore, for most parts, at a rather low level of around 2000 N with the odd peaks reaching maximum warp level, see Figure 5.6. This is also reflected in the PRW model warning signals, see Figure 5.7 where quite few warnings have been triggered. In the second measurement however, the road is more curved and a high constant warp is then applied for nearly the whole measurement, see Figure 5.8. Consequently, in the PRW model output for this measurement a warning is triggered more often than for the first one. The PRW model warning signals for the second measurement can be seen in Figure 5.9.

### 5.3.3 Lane-keeping with warp compensation

The PRW model output with warp compensation for the first measurement can be seen in Figure 5.10. There was not a great deal for the warp compensation algorithm to correct, however still important, most of the warning indicators from the corresponding model simulation without compensation have been removed. More challenging is the second measurement, where constant warp was applied for a longer time and with more force. The PRW model output with compensation can be seen in Figure 5.11. The compensation algorithm seems to
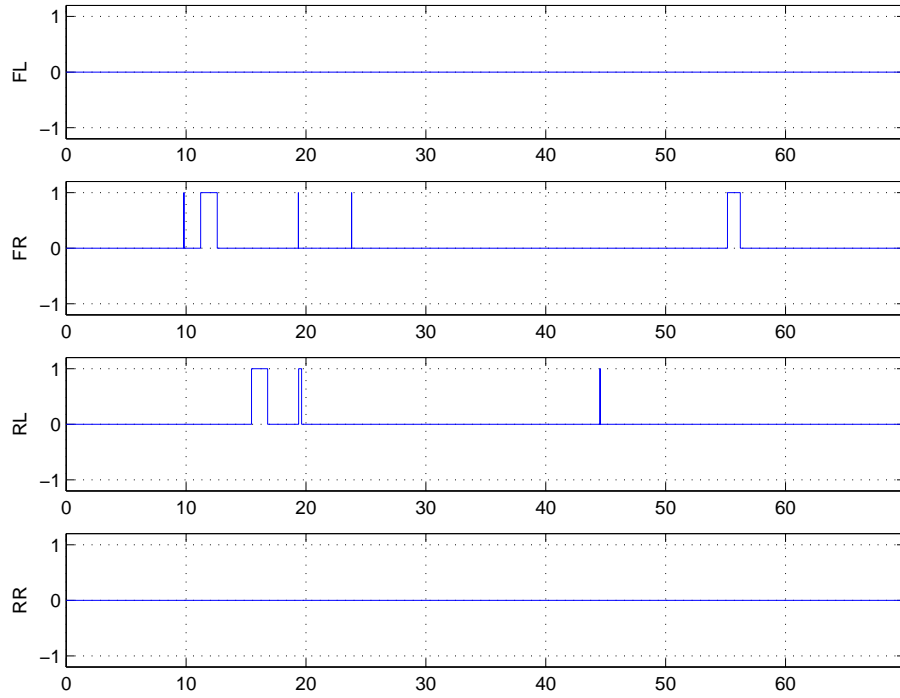
Figure 5.7: PRW model output, without warp compensation, for measurement 1 with lane-keeping application active.
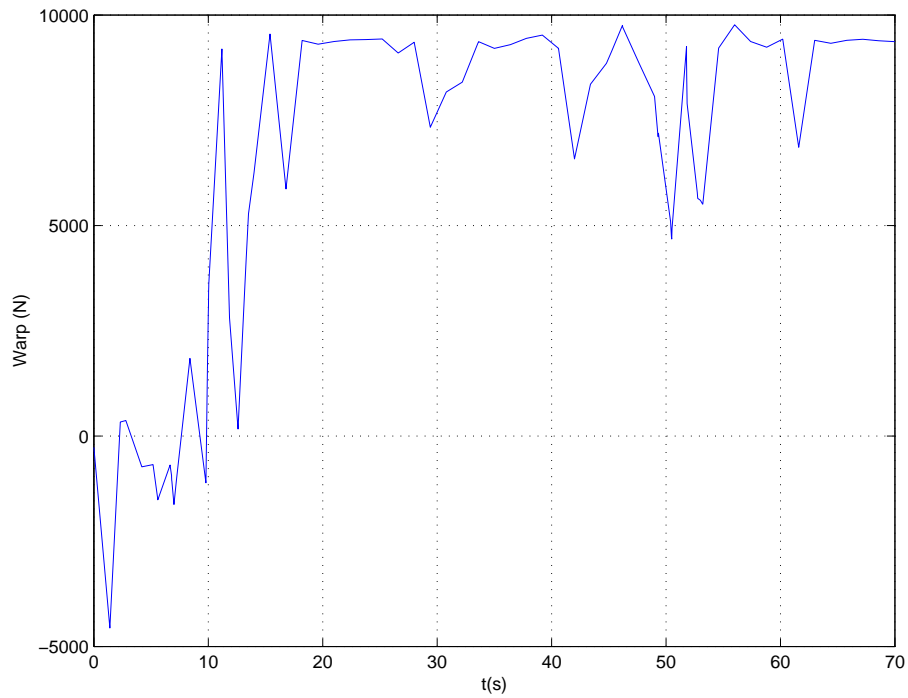


Figure 5.8: Warp force needed for lane-keeping, measurement 2.
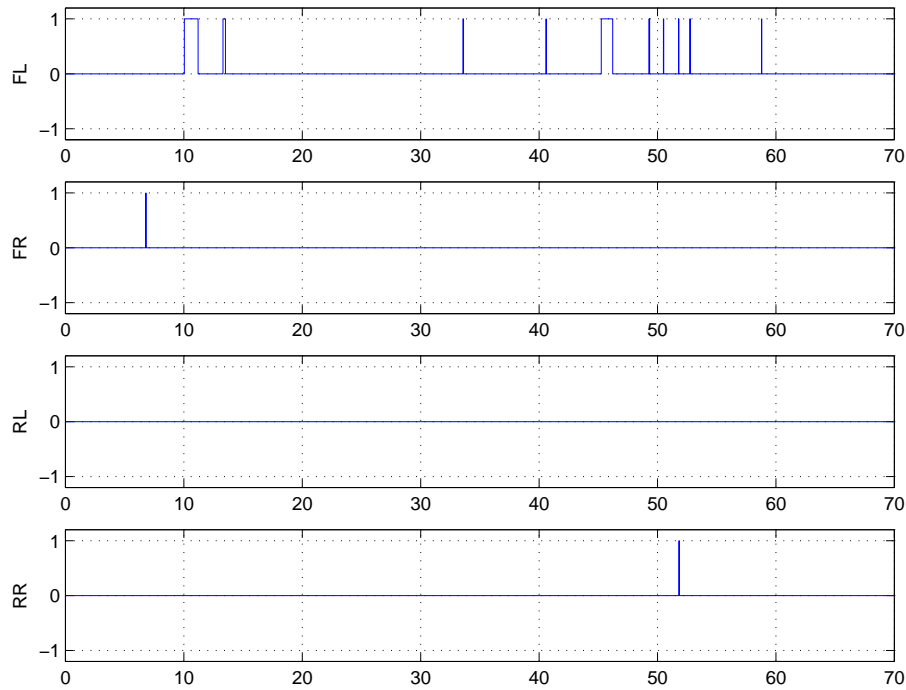
Figure 5.9: PRW model output, without warp compensation, for measurement 2 with lane-keeping application active.

handle also this situation fairly well. Although the occasional high one is still present this is probably not enough to generate a real warning.

## 5.4    Summary

Two applications for warp, road bank assistance and lane-keeping, have been analysed in this chapter in terms of how they affect the functionality of the PRW. These applications are possible candidates for triggering false PRW warnings since a constant warp level is likely to be used in both of them. For the analysis, measurements have been run offline in the simple PRW model introduced in Chapter 4 together with the warp compensation algorithm which gave satisfactory results. For most parts, the compensation was able to suppress the false warnings which were caused by warp.
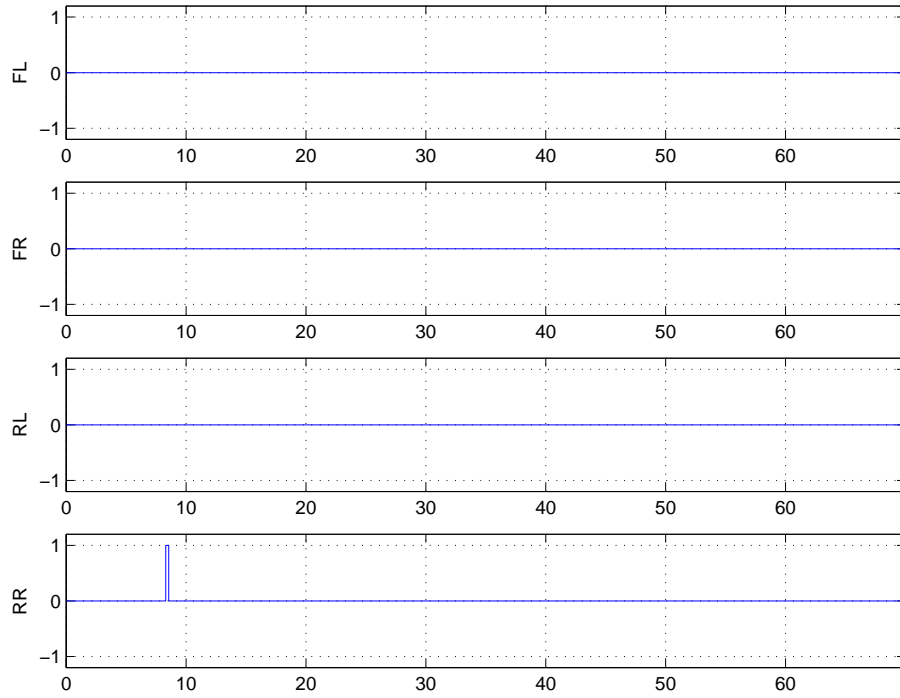
Figure 5.10: PRW model output, with warp compensation, for measurement 1 with lane-keeping application active.
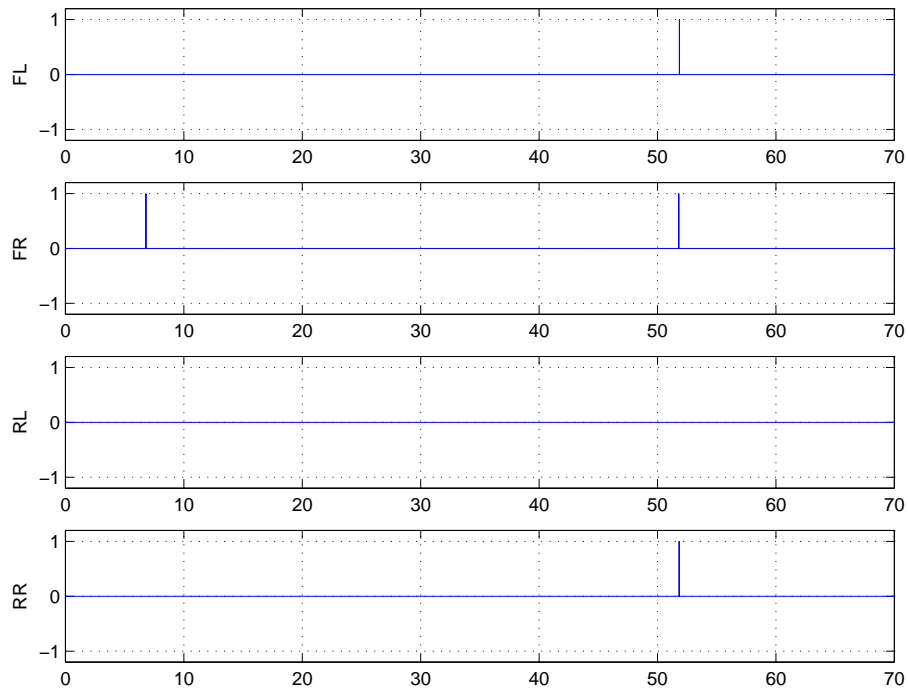


Figure 5.11: PRW model output, with warp compensation, for measurement 2 with lane-keeping application active.

# Chapter 6

# Observation of eigenfrequency of the unsprung mass

## 6.1 The resonance frequency method

A different approach to indirect tyre pressure monitoring, than the method used in the PRW algorithm, involves observation of changes in the dominant eigenfrequencies of the vehicle. The main idea is to transform the appropriate sensor signals into the frequency domain and then to analyse the result in a power spectral density plot.

In order to describe the vertical dynamics of the vehicle, the chassis, the tyres and the suspension system are modelled as a combination of spring-damper systems. When driving, these parts will experience excitation, due to road surface irregularities, which cause vibrations and these vibrations are then present in various sensor signals describing the state of the vehicle. As a result, the different eigenfrequencies belonging to the sprung mass, the suspension and the tyres can be found as some of the dominating frequencies in these signals.

When a tyre is deflated, some of the vehicle's eigenfrequencies are expected to change. This is because the tyre's vertical stiffness (tyre deflection as a function of vertical load) will change with pressure and in turn affect the oscillation of the suspension and everything carried by it. As a result, a possible method for deflation detection is to observe resonance peaks of sensor signals describing the vehicle's current state.

### 6.1.1 Choice of eigenfrequency

As mentioned earlier, there are several different eigenfrequencies which will be affected by a change in tyre pressure and these are therefore possible candidates to use for tyre pressure monitoring purposes. However, all alternatives may not be suitable or even possible to observe, due to filters and sampling frequency.

For this part of the project, measured signals are taken from the ABC system with a sampling frequency of 200 Hz. This restricts the choice of eigenfrequency to observe due to the Nyquist frequency:

$$\omega_N = \frac{\omega_s}{2} \tag{6.1}$$

where $\omega_N$ is the Nyquist frequency, i.e. the highest frequency that can be represented by the sampled data and $\omega_s$ is the sampling frequency.

There is also a hardware lowpass filter present in the system, with a cut-off frequency even lower than 100 Hz, which further limits the choice.

The resonance peak chosen for observation is the one of the suspension/unsprung mass, called the wheel-hop or tyre-hop frequency. This eigenfrequency is located at an adequate frequency, normally at 10-15 Hz, and will be influenced by tyre pressure.

### 6.1.2 The quarter-car model

The quarter-car model is a description of the vehicle's vertical dynamics, see Figure 6.1.
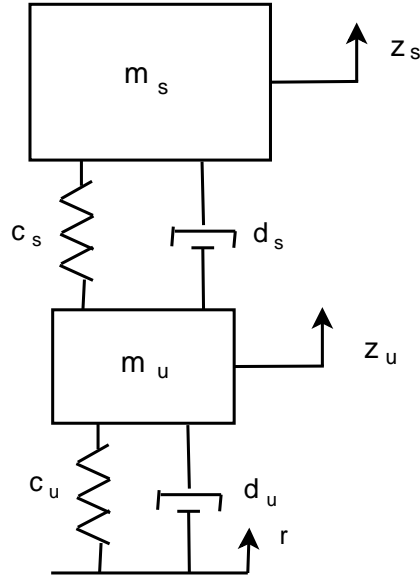


Figure 6.1: The quarter-car model.

The model contains one quarter of the suspended and unsuspended mass, represented by $m_s$ and $m_u$ respectively. The distance travelled by the suspended mass due to road excitation is represented by $z_s$ and the distance travelled by the unsprung mass is referred to as $z_u$. The suspension system, located between the sprung and unsprung mass, is represented by a spring and a damper with the spring/damper constants $c_s$ and $d_s$. The elastic quality of the rubber in the tyre is represented also by a spring and damper, $c_u$ and $d_u$, located between the unsuspended mass and the ground contact point. The input to the system is the road irregularity, $r$.

**Motion equations**

Applying Newton's second law of motion to the quarter-car model gives the following equations [7]:

$$m_s\ddot{z}_s + d_s(\dot{z}_s - \dot{z}_u) + c_s(z_s - z_u) = 0 \qquad (6.2)$$
$$m_u\ddot{z}_u + d_s(\dot{z}_u - \dot{z}_s) + d_u(\dot{z}_u - \dot{r}) + c_s(z_u - z_s) + c_u(z_u - r) = 0 \qquad (6.3)$$

The reference points for the displacements are assumed to be points of static equilibrium for both equations.

**State equations and system matrix**

From now on, the damping constant of the tyre will be set to zero, that is: $d_u = 0$. This simplification is often made and it will not impose any significant restrictions as this constant is fairly small compared to the other constants in the model. In order to derive the system matrix of the model the following state variables are introduced:

$$
\begin{aligned}
x_1 &= z_s \\
x_2 &= \dot{z}_s \\
x_3 &= z_u \\
x_4 &= \dot{z}_u \\
u &= r
\end{aligned}
$$

The first derivative of these state variables are then:

$$
\begin{aligned}
\dot{x}_1 &= x_2 \\
\dot{x}_2 &= -\frac{d_s}{m_s}x_2 - \frac{c_s}{m_s}x_1 + \frac{d_s}{m_s}x_4 + \frac{c_s}{m_s}x_3 \\
\dot{x}_3 &= x_4 \\
\dot{x}_4 &= -\frac{d_s}{m_u}x_4 - \frac{c_s + c_u}{m_u}x_3 + \frac{d_s}{m_u}x_2 + \frac{c_s}{m_u}x_1 + \frac{c_u}{m_u}u
\end{aligned}
$$

This gives the system matrix:

$$
A = \begin{pmatrix}
0 & 1 & 0 & 0 \\
-\frac{c_s}{m_s} & -\frac{d_s}{m_s} & \frac{c_s}{m_s} & \frac{d_s}{m_s} \\
0 & 0 & 0 & 1 \\
\frac{c_s}{m_u} & \frac{d_s}{m_u} & -\frac{(c_s+c_u)}{m_u} & -\frac{d_s}{m_u}
\end{pmatrix}
$$

**Eigenvalues of the system matrix**

If the system matrix is A the eigenvalues $\lambda_i$, $i = 1...n$ for an $n \times n$ matrix, are the solutions to the characteristic equation:

$$
det(\lambda I - A) = 0 \tag{6.4}
$$

The eigenvalue of a system matrix gives rise to an oscillation which can be written as [8]:

$$
\lambda = \sigma + i\omega
$$

where $-\sigma$ is the damping of the oscillation and $|\omega|$ the angular frequency or the eigenfrequency as $\frac{\omega}{2\pi}$.

### 6.1.3 Influence of tyre pressure on the wheel-hop frequency

The eigenfrequencies of the quarter-car model are the resonance frequencies of the sprung and unsprung mass. The system matrix derived in Section 6.1.2 can thus be used to estimate the wheel-hop frequency and, more important, how much this eigenfrequency will change with tyre pressure. A variable in the system matrix is the vertical stiffness constant of the tyre, $c_u$. This value is derived from the relationship between tyre deflection and vertical force. As discussed in Section 3.3, the tyre vertical stiffness changes with tyre pressure as well as tyre make and dimension. Consequently, it is possible to see the influence on the eigenfrequencies of the sprung and unsprung mass due to tyre pressure loss by altering the value of the vertical stiffness constant for the tyre.

The following initial settings for the variables of the quarter-car system matrix will be used when calculating the eigenfrequencies:

- $m_s = 485$ kg

- $m_u = 54$ kg

- $d_s = 2600$ Ns/m

- $c_s = 18000$ N/m

- $c_u = 300000$ N/m

These values are suitable for the Conti 255/40 R19 tyres, which are the front tyres used for the capturing of measurements throughout this project. Thereby, the simulation results obtained here can be used for comparison with the test results which will be presented later in this chapter. The vertical stiffness constant, $c_u$, is estimated from the load-deflection curves in Section 3.3. This value is probably a bit high but it will still provide a good indication for the wheel-hop frequency and how much it will change with tyre pressure.

The wheel-hop frequency is calculated and plotted for a 0-50% change in tyre vertical stiffness and can be seen in Figure 6.2. The initial value is 300 kN/m, for which the wheel-hop frequency has a value of about 11.3 Hz, and then the vertical stiffness constant is gradually decreased, ending at 150 kN/m, 50% of the initial value. Clear from the figure, is that the wheel-hop frequency can be expected to decrease with a decrease in tyre pressure. For a 20% decrease in vertical stiffness, the wheel-hop frequency has reduced about 1.3 Hz, for a 30% decrease the frequency has dropped about 2 Hz and for a 40% decrease the wheel-hop frequency is down at 8.5 Hz, which is a total reduction of 2.8 Hz.

Worth commenting is that a 50% decrease in tyre vertical stiffness is unlikely to be caused by a tyre pressure loss. The results from Section 3.3.2 indicate that the vertical stiffness constant changes around 15-20% for a tyre pressure change of about 25%. But, this relationship is probably not linear meaning that a 50% tyre pressure loss will not result in as much as 40% change in vertical stiffness constant. Thus, a change in wheel-hop frequency due to tyre pressure loss can not be expected to ever be as great as 3.7 Hz which is achieved here for a 50% decrease in tyre vertical stiffness.
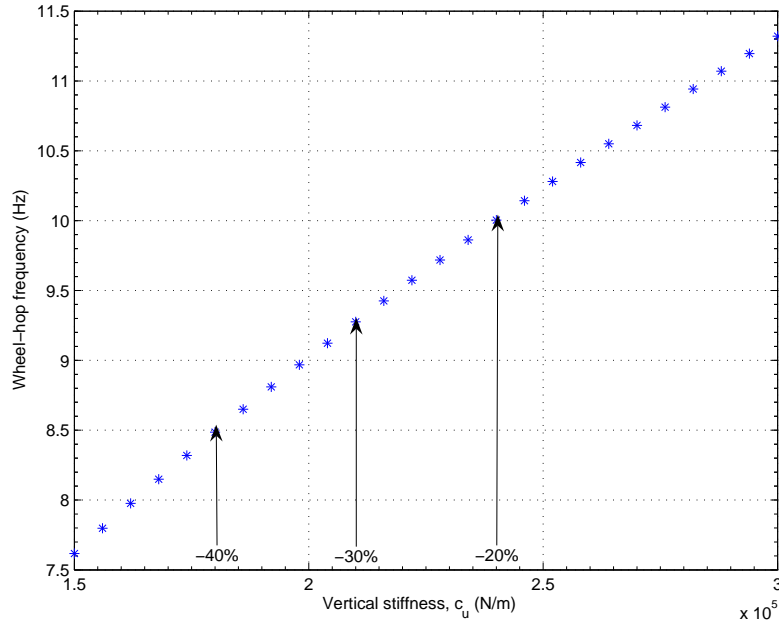
Figure 6.2: The calculated wheel-hop frequency, using the quarter-car system matrix, for different values of tyre vertical stiffness from 300 kN/m to 150 kN/m. The arrows indicate the wheel-hop frequency level for -20, -30 and -40 % of the initial vertical stiffness (300 kN/m).

## 6.2 Spectral analysis

Spectral analysis is used to find the power distribution of a signal over frequency. The result is a Power Spectral Density (PSD) plot. With this description it is possible to see what the dominant frequencies in a signal are.

There are two different approaches for spectral analysis, parametric and non-parametric. Parametric methods interpret the signal as the output of a linear system exited by white noise. The signal is used to estimate the parameters of a model representing the linear system from which the covariance function and spectrum then can be calculated. Non-parametric methods are based solely on the signal itself and are computed with the Fourier transform.

### 6.2.1 The Fourier transform

The Fourier transform translates a continuous time signal $x(t)$ from time domain to frequency domain [8]:

$$X(f) = \int_{-\infty}^{\infty} e^{i2\pi ft} x(t) dt \tag{6.5}$$

The result is an infinite number of frequency components, $X(f)$.

For a finite sequence of length $N$ of a sampled signal, $x(n)$, the Discrete Fourier Transform (DTF) must be used. This produces a finite number of frequency samples, $X(k)$ as [9]:

$$X(k) = \sum_{n=0}^{N-1} e^{\frac{-i2\pi}{N}kn} x(n) \tag{6.6}$$

Computation of the Discrete Fourier Transform is very demanding and for this reason the Fast Fourier Transform (FFT) is used for implementation purposes which reduces the computational time from $2N^2$ to $2Nlog_2N$.

## 6.2.2 The periodogram

The periodogram is a non-parametric method which is used to estimate the spectral density of a signal. It is calculated by taking the squared magnitude of the Discrete Fourier Transform of each signal sample. For a limited sequence of data points, $x_N(n)$, the N-point periodogram, $R_N(k)$, is defined as [10]:

$$\begin{aligned} R_N(k) &= \frac{1}{N}|X_N(k)|^2 \\ &= \frac{1}{N}|\sum_{n=0}^{N-1} e^{\frac{-i2\pi}{N}kn} x(n)|^2 \end{aligned} \tag{6.7}$$

**Variance**

The periodogram is asymptotically unbiased. If an infinite number of data points $N$ are used the estimate approaches the true value. However, it is not consistent, meaning that the variance does not decrease with $N$. Therefore, averaging must be introduced to reduce variance. The data is split into $k$ segments, for each segment the periodogram is calculated and finally an average of the $k$ periodograms is taken. The variance decreases linearly with $k$ but introduces a bias due to worsened resolution. For a too high $k$ the frequency peaks will be unclear and thus there is a trade-off between reducing variance and introducing bias.

**Spectral leakage**

For the computation of the periodogram, an infinite signal is sampled and $N$ points chosen, resulting in the N-point periodogram. Selecting the $N$ points is the same as multiplying the infinite sequence of samples, $x(n)$ with a rectangular function:

$$x_N(n) = x(n)w_R(n)$$

Transforming from time domain to frequency domain results in the convolution:

$$x_N(k) = \int_{-f_s/2}^{f_s/2} x(\rho)w_R(f-\rho)d\rho$$

Again, the N-point periodogram PSD estimate is:

$$R_N(k) = \frac{|x_N(k)|^2}{N}$$

and will thus be affected by the introduction of the window function due to the limitation of having to use finite data sequences.

To reduce the effect of spectral leakage, the data sequence can be multiplied with a window function which has better properties than the rectangular window. There are many different window functions available, the desirable properties are well suppressed side lobes to prevent leakage and a narrow main lobe for good resolution.

**Modified periodogram**

The modified periodogram divides the data sequence into several segments and a window function is applied to each one. The Fourier transform is then applied to each segment and an average is computed.

## 6.3   Validation of method

In this section, the possibilities of the eigenfrequency method as a tyre deflation monitoring system will be investigated. It is necessary to see how well low tyre pressure can be detected, before trying to use the method when driving with warp. Therefore, first of all, measurements from driving straight ahead on a test track with normal pressure on all tyres will be compared with driving on the same track with one tyre deflated.

### 6.3.1   Choice of signals for observation

To be able to use observation of the wheel-hop frequency for tyre pressure monitoring purposes, it is desirable to find the signals where this frequency is dominant and therefore visible in a power spectral density plot. The sensor signals that are presumed to fulfill this condition and that will be investigated are:

- Acceleration of the sprung mass, $\ddot{x}_s$.

- Difference in vertical distance travelled by the sprung and unsprung mass, $x_s - x_u$.

- Wheel load, vertical force at the wheel, $Fz_u$.

- Pressure in cylinder belonging to the active suspension system, one for each wheel.

- Angular wheel speed, $\omega_i$, $i = 1, 2, 3, 4$.

### 6.3.2   Road surface

The road irregularities, the input signal to the quarter-car model, have a great impact on the performance of this method. The road surface needs to have the right amount of roughness such that the vertical movement of the vehicle will be exited enough for the wheel-hop frequency to show well but still not too bumpy since then the spectrum plot will be unclear. With the purpose to find the ideal road conditions, spectrum analyses with measurements from three different types of track surface have been made: normal road (asphalt), rough road (uneven asphalt with some gravel) and track with evenly spaced road bumps.

The most useful track, out of these three, turned out to be the normal asphalt road. The other two types of road surface seemed to induce too strong oscillations of the vehicle body

and suspension, resulting in most of the spectrum plots for measurements from these surfaces not showing a clear peak at the wheel-hop frequency, which is a prerequisite for using the eigenfrequency method at all. One example of a spectrum plot for the vertical acceleration from the track with road bumps can be seen in Figure 6.3. The problem with this type of result is that it is very hard to determine which peak belongs to the wheel-hop frequency which makes it very difficult to use for tyre pressure monitoring purposes.
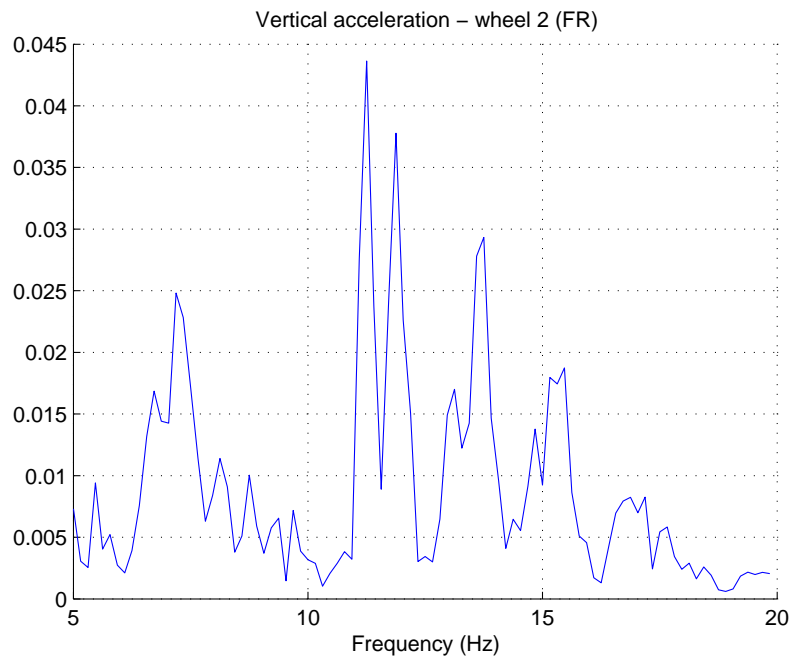


Figure 6.3: Spectral analysis of vertical acceleration signal from a measurement captured when driving on track with road bumps. Velocity was 80 km/h.

### 6.3.3 Test results

The results presented here are all spectrum plots for measurements captured on a normal asphalt road as the wheel-hop frequency appears fairly well in these measurements for some signals and therefore this seemed to be a suitable road track. One example of a spectral plot of a vertical acceleration signal for a measurement captured on a normal road can be seen in Figure 6.4.

Comparing with the spectral plot of the vertical acceleration from the measurement from the bumpy road, it is clear that this surface gives a better result. Also, the eigenfrequency peak is located at around 11 Hz which coincides with what was predicted in Section 6.1.3.

There is one major issue with the results for this method of tyre pressure monitoring. It proved to be very difficult to see a change in the wheel-hop frequency in the captured measurements with change in tyre pressure. Again, referring to Section 6.1.3, it was established that the wheel-hop frequency should be located at about 11 Hz and that a lower tyre pressure should move the eigenfrequency down about 1-2 Hz – depending on the change in vertical stiffness caused by the lower pressure. This movement of the wheel-hop frequency has not
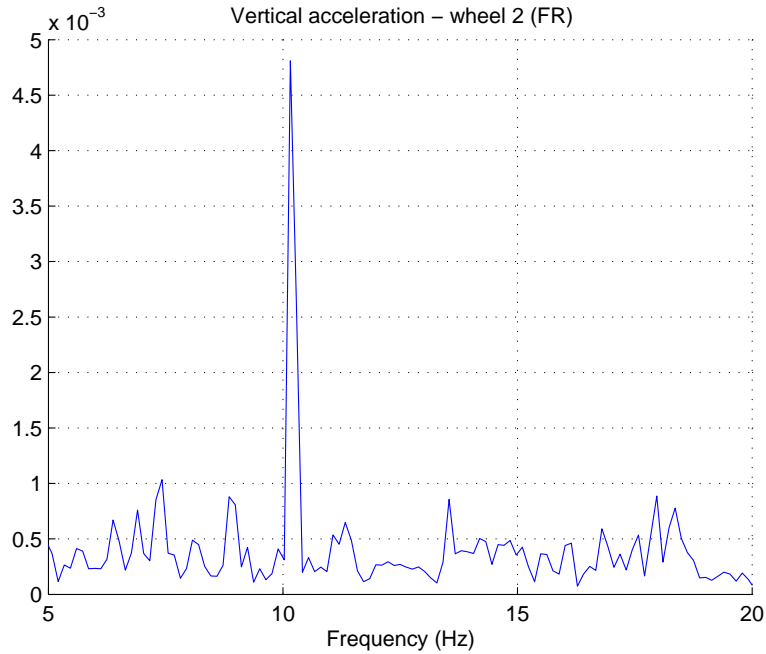
Figure 6.4: Spectral analysis of vertical acceleration signal from a measurement captured when driving on a normal asphalt road. Velocity was 80 km/h.

been clear in any of the measurements captured. The change has been very small, and some of the time even undetectable.

One example can be seen in Figure 6.5 where the spectrum plot of the vertical acceleration of the body at wheel 2 (FR) for two different tyre pressures can be seen. The spectrum from the lower pressure measurement, 1.5 bar, gives rise to a lower amplitude, which it should, but is located at almost exactly the same frequency as the spectrum from the measurement with the normal pressure level, 2.8 bar. The same phenomenon can be seen in the other signals from the same measurement. Two examples are the wheel load signal, $Fz_u$, in Figure 6.6 and the signal describing the difference in vertical distance travelled by the sprung and unsprung mass, $x_s - x_u$ in Figure 6.7.

Since the different signals in most of the measurements provide similar results, no further presentation of the results obtained will be made here.
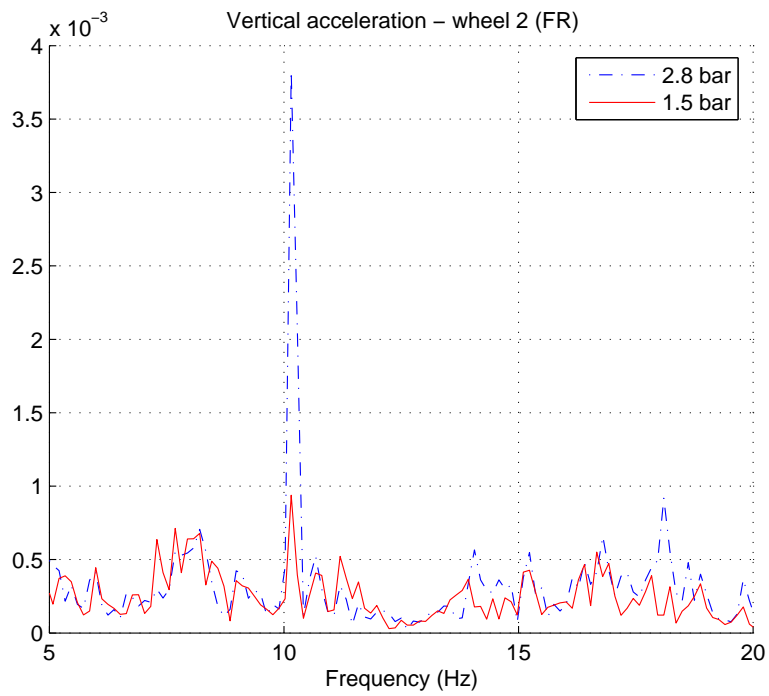
Figure 6.5: Spectral analysis of vertical acceleration signal for wheel 2 (FR). One measurement with all tyres at 2.8 bar (dotted line) and one measurement (solid line) with wheel 2 about 50% deflated, 1.5 bar.

Figure 6.6: Spectral analysis of wheel load signal for wheel 2 (FR). One measurement with all tyres at 2.8 bar (dotted line) and one measurement (solid line) with wheel 2 about 50% deflated, 1.5 bar.



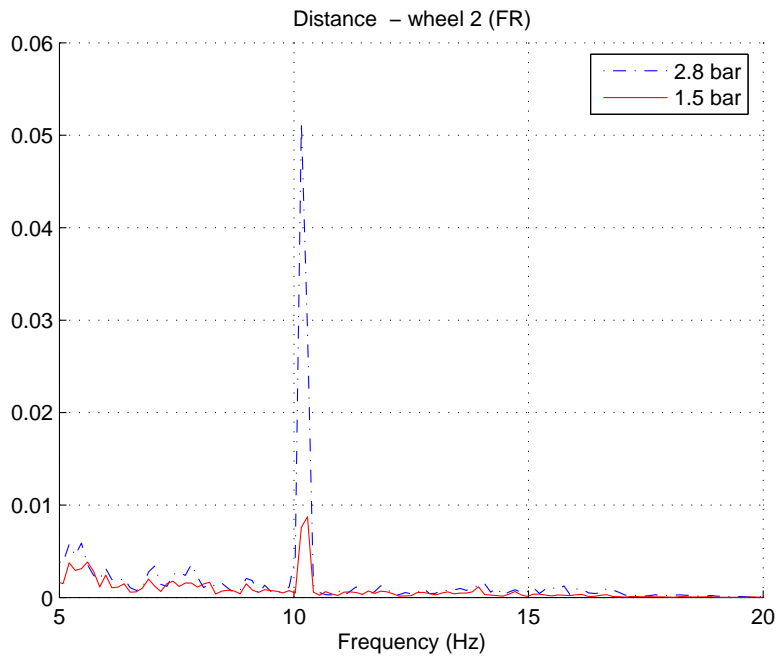Figure 6.7: Spectral analysis of signal describing the difference in vertical distance travelled by the sprung and unsprung mass for wheel 2 (FR). One measurement with all tyres at 2.8 bar (dotted line) and one measurement (solid line) with wheel 2 about 50% deflated, 1.5 bar.

## 6.4 Summary

In this section, observation of the eigenfrequency of the unsprung mass was presented as a method for tyre deflation warning. The quarter-car system matrix, together with the results presented earlier about change in vertical stiffness due to tyre pressure, indicated that the wheel-hop frequency changes with tyre pressure and should therefore be possible to monitor. Unfortunately no change in the eigenfrequency could be found in any of the measurements captured for this project. The reason for this problem is uncertain but could have something to do with the sensors that provide the signals that were analysed or the spectral analysis method. Due to the poor results, the eigenfrequency method was not further investigated to analyse the possibilities as a monitoring system when driving with warp.

# Chapter 7

# Conclusions and future work

## 7.1 Conclusions

The goal for this thesis was to analyse the influence by warp on the tyre pressure monitoring system, the PRW, present in some of the Mercedes cars. The PRW issues false warnings when driving with, especially, constant warp and it is desirable that this should be prevented.

Chapter 2 presented the PRW algorithm in detail. There it was established that the PRW warning system is based on the values of three variables: *diag*, *fr* and *lr* which are composed of the angular wheel speeds of the vehicle. If a tyre is deflated, the variables will change such that a warning condition is fulfilled. The *diag* variable is actually the tyre deflation indicator, but the other two variables are needed to prevent false warnings.

Warp alters the wheel loads of the vehicle which will affect the dynamic radius of all tyres and therefore also the wheel speeds. Consequently, the PRW variables, especially *diag*, will change due to warp and, as was concluded in Chapter 3, this will cause false warnings. How the dynamic radius changes with wheel load depends on the tyre vertical stiffness and, as was also established in Chapter 3, the vertical stiffness is dependent on several factors including tyre make and dimension. Therefore, a compensation method which will suit all tyres available can be difficult to design.

In Chapter 4, a compensation algorithm for warp was presented and tried offline with field measurements. The algorithm is based on the relationship between the PRW variable *diag* and warp. Although it seemed to be able to suppress the influence by warp, the question is still if it would work for other tyres than it was developed for. In one small experiment, the compensation algorithm was run using one measurement captured with different set of tyres than used in all other tests. This experiment gave promising results but can not be viewed as a guarantee that the algorithm works for all tyres without adapting the settings. The algorithm however seems to have potential, which was showed in Chapter 5. There it was analysed, again offline, with some measurements captured during two applications for warp: road bank assistance and lane-keeping. The compensation algorithm was able to suppress the influence of the PRW variable *diag* by warp.

An alternative tyre pressure monitoring system which is based on observing sensor signals in the frequency domain was investigated in Chapter 6. There, an attempt to monitor the eigenfrequency of the unsprung mass, the wheel-hop frequency, was made. The results were not successful in the sense that the presumed change in the wheel-hop frequency could not be seen in any of the signals in the measurements which were captured for this part of the project.

## 7.2 Future work

The warp compensation algorithm presented in Chapter 4 and further tried in Chapter 5 has only been analysed with measurements offline. To get a more assuring indication if the algorithm would work properly, it is necessary to run it online in the vehicle. Also, the algorithm was run together with a simplified model of the PRW and has only been exposed to gentle driving in the sense that no acceleration, braking or cornering were present in the measurements. All in all, the warp compensation needs to be further analysed online in more realistic driving situations before it is possible to establish if it is a working algorithm.

Also, the robustness of the algorithm with respect to other tyres than the ones used for development of this algorithm must be investigated. The compensation must be compatible with all types of tyres, that is, all possible values of tyre vertical stiffness. One solution to this problem does not actually have to involve changing the compensation algorithm. Estimating the lateral stiffness, which is correlated to the vertical stiffness, can be used to decide which tyre has been fitted and thus decide the settings that correspond to the particular tyres which can then be used in the compensation algorithm. Using this type of tyre estimation in combination with the warp compensation algorithm is a possible solution to the issue of different vertical stiffness which would be worth investigating.

# Bibliography

[1] Vägverket
    Available at: www.vv.se
    November 2006

[2] Winfried Gaal, Infineon Technologies AG
    *Surface Micro Machined Sensor Technology for Future Tire Pressure Monitoring Systems (TPMS)*
    Proceedings 2nd VDE World Microtechnologies Congress, 2003 pp.435-438

[3] *PRW Software Description*
    Supplied by Daimler Chrysler

[4] Prof. Dr. Georg Rill
    *Vehicle Dynamics, Lecture Notes*
    Fachhochschule Regensburg, University of Applied Sciences

[5] Thomas Merker, Gaston Girres, Olaf Thriemer
    *Active Body Control (ABC) The DaimlerChrysler Active Suspension and Damping System*
    Proceedings 2002 International Congress on Transportation Electronics pp.363-369

[6] *Continental, Technical Databook 2005-2006*
    Available from: http://www.conti-online.com/generator/www/de/en/
    continental/automobile/themes/tyretips/technischer_ratgeber/
    technical_databook_en.html
    January 2007

[7] Prof. Dr.-Ing C. Woernle
    *Fahrmechanik, Lecture Slides*
    Universität Rostock, Lehrstuhl für Technische Dynamik

[8] Sven Spanne
*Lineära System*, Third edition
KFS 1995

[9] Sven Spanne
*Konkret Analys*, Third edition
KFS 1995

[10] G. Lindgren, H. Rootzén
*Stationära Stokastiska Processer*, Fourth edition
KFS 2005